DISCRETE GRADIENT FLOWS FOR GENERAL CURVATURE ENERGIES*

WILLY DÖRFLER† AND ROBERT NÜRNBERG‡

Abstract. We consider the numerical approximation of the L^2–gradient flow of general curvature energies $\int G(|\vec{\varkappa}|)$ for a curve in $\mathbb{R}$, $d \geq 2$. Here the curve can be either closed, or it can be open and clamped at the end points. These general curvature energies, and the considered boundary conditions, appear in the modeling of the power loss within an optical fiber. We present two alternative finite element approximations, both of which admit a discrete gradient flow structure. Apart from being stable, in addition, one of the methods satisfies an equidistribution property. Numerical results demonstrate the robustness and the accuracy of the proposed methods.

Key words. curvature energy, gradient flow, clamped boundary conditions, finite element approximation, equidistribution, optical fiber

AMS subject classifications. 65M60, 65M12, 35K55, 53C44, 74E10

DOI. 10.1137/18M122844X

1. Introduction.

The classical elastic energy of a curve is defined by the integral of the squared norm of the curvature vector $\vec{\varkappa}$. This energy, as a model for the elastic energy of a rod, has been first considered and analyzed by Bernoulli (1738) and Euler (1743); see [17]. Further, and more recent, applications for this energy are the modeling of DNA rings and other curved nanostructures (see [18, 28]) and edge completion in computer vision; see [22].

In this paper we study the L^2–gradient flow of curvature energies that depend in a more general form on $\vec{\varkappa}$. Such energies appear, for example, when one studies the power loss within an optical fiber that acts as a wire bond, i.e., as an interchip connection, where data is transmitted by light between different components of the chip; see [20]. Since these connections are long and thin, a common modeling approach is to formulate the losses in terms of geometrical quantities of a connecting curve. More specifically, the energy we are going to consider is defined by

$$(1.1) \qquad \int [G(|\vec{\varkappa}|) + \lambda],$$

where $G(|\kappa|)$ is the optical loss per length due to the bending of the wire bond, while $\lambda > 0$ models the optical loss per length of the connection. If P_{in} and P_{out} denote the incoming and outgoing power, respectively, then the loss in this model is given by

$$(1.2) \qquad \frac{P_{\text{in}} - P_{\text{out}}}{P_{\text{in}}} = 1 - \exp\left(-2 \int [G(|\vec{\varkappa}|) + \lambda]\right),$$

and so minimizing the loss is equivalent to minimizing the energy (1.1). Examples for functions G of interest are

$$G(z) = \tfrac{1}{p}\, z^p\,, \qquad p \in (1, \infty)\,, \tag{1.3a}$$

$$G(z) = e^{-\alpha/z}\,, \qquad \alpha \in (0, \infty)\,, \tag{1.3b}$$

$$G(z) = \sqrt{z}\, e^{-\alpha/z}\,, \quad \alpha \in (0, \infty)\,. \tag{1.3c}$$

The case (1.3a) with $p = 2$ leads to the classical elastic energy, while a physical interpretation for (1.3a) with $p \in (1, \infty)$ in connection with losses in optical fibers is given in [1, eq. (16)] and [19, p. 819] ($d = 2$). The choices (1.3b)–(1.3c) are in the same connection advocated in [21, eq. (14)] for $d = 2$ and in [21, eq. (34)] for $d = 3$. While these (approximative) formulas were originally derived for constantly curved slabs or fibers, they are also used for trajectories with slowly varying curvature. In applications one would provide two contact points for the wire, and a prescribed direction for the wire at each endpoint. These boundary conditions are called "clamped boundary conditions." A more realistic model of wire bonds would include also the "transition loss" caused by varying curvature in (1.2). However, a corresponding term in the energy (1.1) that models the transition loss is not known to this date. In [23] such a wire bond connection in the plane was optimized with respect to its loss by using (1.1), but with transition losses calculated from the interpolation of precomputed values. In this paper we will neglect transition losses and concentrate on (1.1) instead.

Of course, for the choice (1.3a) with $p = 2$ the energy (1.1) reduces to the classical elastic energy, and its L^2–gradient flow is called elastic flow. The classical case is by now well studied both analytically and numerically. For theoretical results we refer to [24, 16, 11, 12, 25, 7], while numerical approximations have been considered in [16, 9, 2, 4]. Schemes for the elastic flow of inextensible curves have been proposed and analyzed in [5, 6]. Here we stress that in [9] a first stability result for a discretization of elastic flow was presented, together with an error analysis. In [4] an alternative discretization was presented that can also be shown to be stable and that, in addition, satisfies an equidistribution property.

It is the aim of this paper to extend the stability results in [9, 4] to the more general energy (1.1). In applications one is often interested in the minimizing shape of the curve. Here we view the L^2–gradient flow as an opportune method to produce possible candidates. We stress that, to the best of our knowledge, so far there exist no results on the analysis or numerical analysis of gradient flows for the more general energy (1.1). Moreover, we will present exact radial solutions for the L^2-gradient flow of (1.1) for the choices in (1.3). Once again, we believe that these are the first such results in the literature. Finally, we remark that our theoretical and numerical results reveal the qualitatively very different behavior of the evolution for the gradient flow for general G, compared to the classical case, when $G(z) = \tfrac{1}{2} z^2$. For example, while stationary solutions exist for (1.3a) for any $p \in (1, \infty)$ and $\lambda > 0$, there are no stationary solutions in the cases (1.3b) and (1.3c) if λ is sufficiently large.

The remainder of this paper is organized as follows. In the next section we introduce the precise mathematical formulations of the gradient flows we would like to study. In section 3 we state two alternative weak formulations, and in section 4 we introduce continuous-in-time semidiscrete finite element approximations based on these formulations. We show that our approximations satisfy a stability bound and prove an equidistribution property for one of the schemes. In section 5 we introduce

the corresponding fully discrete versions of the semidiscrete approximations derived in the previous section. At every time level, a nonlinear system has to be solved for the approximations, and we give details on a possible solution procedure. In section 6 we report on numerous numerical experiments, which demonstrate the effectiveness of our fully discrete approximations. Moreover, convergence experiments, based on exact solutions that we derive in the appendix, show a quadratic convergence rate for our finite element approximations.

2. Mathematical formulation. Let either $I = \mathbb{R}/\mathbb{Z}$, the periodic interval $[0, 1]$, or $I = (0, 1)$. Note that in the former case we have $\partial I = \emptyset$, while in the latter case it holds that $\partial I = \{0, 1\}$. Let $\vec{x} : \bar{I} \to \mathbb{R}^d$ be a parametrization of the curve $\Gamma \subset \mathbb{R}^d$, $d \geq 2$. Note that Γ is closed if $I = \mathbb{R}/\mathbb{Z}$ and open if $I = (0, 1)$. We also define the function spaces $\underline{V} = [H^1(I)]^d$ and $\underline{W} = [H_0^1(I)]^d$, and note that $\underline{W} = \underline{V}$ in the case $I = \mathbb{R}/\mathbb{Z}$.

On assuming that

$$(2.1) \qquad |\vec{x}_\rho(\rho)| \geq c_0 > 0 \qquad \forall \, \rho \in I \,,$$

we introduce the arclength parameter s of the curve, i.e., $\partial_s = |\vec{x}_\rho|^{-1} \, \partial_\rho$, and define the unit tangential vector field

$$(2.2) \qquad \vec{\tau}(\rho) = \vec{x}_s(\rho) = \frac{\vec{x}_\rho(\rho)}{|\vec{x}_\rho(\rho)|} \,.$$

When we consider the evolution of open curves, we impose the clamped boundary conditions

$$(2.3) \qquad \vec{x}(q) = \vec{\alpha}_q \quad \text{and} \quad (-1)^{q+1} \, \vec{\tau}(q) = \vec{\zeta}_q \quad \forall \, q \in \partial I \,,$$

for given $\vec{\alpha}_0, \vec{\alpha}_1 \in \mathbb{R}^d$ and $\vec{\zeta}_0, \vec{\zeta}_1 \in \mathbb{S}^{d-1} = \{\vec{p} \in \mathbb{R}^d : |\vec{p}| = 1\}$. The curvature vector $\vec{\varkappa}$ of Γ is given by

$$(2.4) \qquad \vec{\varkappa} = \vec{\tau}_s = \vec{x}_{ss} \,, \quad \text{implying} \quad \vec{\varkappa} \cdot \vec{\tau} = 0 \,.$$

Energy minimization. We are interested in minimizers of the energy

$$(2.5) \qquad E_\lambda(\vec{x}) = \int_I \left[G(|\vec{\varkappa}|) + \lambda \right] |\vec{x}_\rho| \, \mathrm{d}\rho \,,$$

where $\lambda \in \mathbb{R}$ is a constant, subject to the boundary conditions (2.3), and with given energy density $G : \mathbb{R}_{\geq 0} \to \mathbb{R}_{>0}$. Variations of (2.5) in $\vec{\varkappa}$ in the direction of a vector field $\vec{\eta}$, yield the term $\int_I G'(|\vec{\varkappa}|) \, |\vec{\varkappa}|^{-1} \, \vec{\varkappa} \cdot \vec{\eta} \, |\vec{x}_\rho| \, \mathrm{d}\rho$, and so unless there are further conditions on G, this term does not make sense for $\vec{\varkappa} \to \vec{0}$. A sufficient condition for this term to be well defined is

$$(2.6) \qquad G'(z) \to 0 \text{ as } z \to 0 \,,$$

and we make that assumption from now on. Note that it is satisfied for the examples (1.3a)–(1.3c). Throughout this paper, we set $G'(|\vec{z}|) \, |\vec{z}|^{-1} \, \vec{z} = \vec{0}$ if $\vec{z} = \vec{0}$, which is justified by (2.6).

Gradient flow. In order to approach stationary points of (2.5) we will use a time dependent gradient flow. We begin by deriving the strong formulation of the L^2-gradient flow of (2.5). To this end, let $(\Gamma(t))_{t \in [0,T]}$ be a family of curves in $\mathbb{R}^d$, parameterized by $\vec{x} : \overline{I} \times [0,T] \to \mathbb{R}^d$, $(\rho, t) \mapsto \vec{x}(\rho, t)$. Straightforward calculations give, on recalling (2.4), that

$$(2.7) \qquad (|\vec{x}_\rho|)_t = \vec{x}_s \cdot (\vec{x}_t)_\rho = \vec{\tau} \cdot (\vec{x}_t)_\rho \,, \qquad \vec{\tau}_t = |\vec{x}_\rho|^{-1} \, \underline{P} \, \vec{x}_{\rho, t} = \vec{\nabla}_s \, \vec{x}_t \,,$$

where the normal projection $\underline{P}$ is defined by

$$(2.8) \qquad \underline{P} = \underline{\mathrm{Id}} - \vec{\tau} \otimes \vec{\tau} \quad \text{and} \quad \vec{\nabla}_s = \underline{P} \, \partial_s \,.$$

A weak formulation of (2.4), on noting (2.3), is given by

$$(2.9) \qquad \int_I \vec{\varkappa} \cdot \vec{\eta} \, |\vec{x}_\rho| \, \mathrm{d}\rho + \int_I \vec{\tau} \cdot \vec{\eta}_\rho \, \mathrm{d}\rho = \sum_{q \in \partial I} \vec{\zeta}_q \cdot \vec{\eta}(q) \qquad \forall \, \vec{\eta} \in \underline{V} \,.$$

Note that $\vec{\eta}(q)$ is well defined for $\vec{\eta} \in [H^1(I)]^d$. Differentiating (2.9) with respect to time yields

$$(2.10) \qquad \int_I \vec{\varkappa}_t \cdot \vec{\eta} \, |\vec{x}_\rho| \, \mathrm{d}\rho + \int_I \vec{\varkappa} \cdot \vec{\eta} \, (|\vec{x}_\rho|)_t \, \mathrm{d}\rho + \int_I \vec{\tau}_t \cdot \vec{\eta}_\rho \, \mathrm{d}\rho = 0 \qquad \forall \, \vec{\eta} \in \underline{V} \,.$$

It follows from (2.10) and (2.7), and on assuming the boundary conditions (2.3), that

$$\frac{\mathrm{d}}{\mathrm{d}t} E_\lambda(\vec{x}) = \frac{\mathrm{d}}{\mathrm{d}t} \int_I [G(|\vec{\varkappa}|) + \lambda] \, |\vec{x}_\rho| \, \mathrm{d}\rho$$

$$= \int_I G'(|\vec{\varkappa}|) \, |\vec{\varkappa}|^{-1} \, \vec{\varkappa} \cdot \vec{\varkappa}_t \, |\vec{x}_\rho| \, \mathrm{d}\rho + \int_I [G(|\vec{\varkappa}|) + \lambda] \, (|\vec{x}_\rho|)_t \, \mathrm{d}\rho$$

$$= -\int_I [G'(|\vec{\varkappa}|) \, |\vec{\varkappa}|^{-1} \, \vec{\varkappa}]_\rho \cdot \vec{\tau}_t \, \mathrm{d}\rho + \int_I \left[G(|\vec{\varkappa}|) - G'(|\vec{\varkappa}|) \, |\vec{\varkappa}| + \lambda \right] (|\vec{x}_\rho|)_t \, \mathrm{d}\rho$$

$$= -\int_I \left(\underline{P} \, [G'(|\vec{\varkappa}|) \, |\vec{\varkappa}|^{-1} \, \vec{\varkappa}]_s - \left[G(|\vec{\varkappa}|) - G'(|\vec{\varkappa}|) \, |\vec{\varkappa}| + \lambda \right] \vec{\tau} \right) \cdot (\vec{x}_t)_\rho \, \mathrm{d}\rho$$

$$(2.11) \qquad = \int_I \left(\underline{P} \, [G'(|\vec{\varkappa}|) \, |\vec{\varkappa}|^{-1} \, \vec{\varkappa}]_s - \left[G(|\vec{\varkappa}|) - G'(|\vec{\varkappa}|) \, |\vec{\varkappa}| + \lambda \right] \vec{\tau} \right)_s \cdot \vec{x}_t \, |\vec{x}_\rho| \, \mathrm{d}\rho \,.$$

Hence the strong form of the L^2-gradient flow of (2.5), subject to (2.3), is given by

$$(2.12) \qquad \vec{x}_t = -\left(\underline{P} \, [G'(|\vec{\varkappa}|) \, |\vec{\varkappa}|^{-1} \, \vec{\varkappa}]_s \right)_s + \left([G(|\vec{\varkappa}|) - G'(|\vec{\varkappa}|) \, |\vec{\varkappa}| + \lambda] \, \vec{\tau} \right)_s \,.$$

On noting from (2.8), $\vec{\tau}_s \cdot \vec{\tau} = 0$, and (2.4) that

$$\vec{\nabla}_s^2 \left(G'(|\vec{\varkappa}|) \, |\vec{\varkappa}|^{-1} \, \vec{\varkappa} \right) = \left[\vec{\nabla}_s \left(G'(|\vec{\varkappa}|) \, |\vec{\varkappa}|^{-1} \, \vec{\varkappa} \right) \right]_s - \left(\left[\vec{\nabla}_s \left(G'(|\vec{\varkappa}|) \, |\vec{\varkappa}|^{-1} \, \vec{\varkappa} \right) \right]_s \cdot \vec{\tau} \right) \vec{\tau}$$

$$= \left[\vec{\nabla}_s \left(G'(|\vec{\varkappa}|) \, |\vec{\varkappa}|^{-1} \, \vec{\varkappa} \right) \right]_s + \left[G'(|\vec{\varkappa}|) \, |\vec{\varkappa}|^{-1} \, \vec{\varkappa} \right]_s \cdot \vec{\tau}_s \, \vec{\tau}$$

$$= \left[\vec{\nabla}_s \left(G'(|\vec{\varkappa}|) \, |\vec{\varkappa}|^{-1} \, \vec{\varkappa} \right) \right]_s + \left[G'(|\vec{\varkappa}|) \, |\vec{\varkappa}|^{-1} \right]_s \, |\vec{\varkappa}|^2 \, \vec{\tau} + G'(|\vec{\varkappa}|) \, |\vec{\varkappa}|^{-1} \, (\vec{\varkappa}_s \cdot \vec{\varkappa}) \, \vec{\tau}$$

$$= \left[\vec{\nabla}_s \left(G'(|\vec{\varkappa}|) \, |\vec{\varkappa}|^{-1} \, \vec{\varkappa} \right) \right]_s + [G'(|\vec{\varkappa}|)]_s \, |\vec{\varkappa}| \, \vec{\tau} \,,$$

we can rewrite (2.12) as

$$\vec{x}_t = -\left[\vec{\nabla}_s\left[G'(|\vec{\varkappa}|)\,|\vec{\varkappa}|^{-1}\,\vec{\varkappa}\right]\right]_s + \left[G(|\vec{\varkappa}|) - G'(|\vec{\varkappa}|)\,|\vec{\varkappa}|\right]_s\vec{\tau}$$
$$+ \left[G(|\vec{\varkappa}|) - G'(|\vec{\varkappa}|)\,|\vec{\varkappa}| + \lambda\right]\vec{\varkappa}$$
$$= -\vec{\nabla}_s^2\left(G'(|\vec{\varkappa}|)\,|\vec{\varkappa}|^{-1}\,\vec{\varkappa}\right) + \left[G(|\vec{\varkappa}|) - G'(|\vec{\varkappa}|)\,|\vec{\varkappa}| + \lambda\right]\vec{\varkappa}$$
$$+ \left[G(|\vec{\varkappa}|) - G'(|\vec{\varkappa}|)\,|\vec{\varkappa}|\right]_s\vec{\tau} + \left[G'(|\vec{\varkappa}|)\right]_s|\vec{\varkappa}|\,\vec{\tau}$$
$$= -\vec{\nabla}_s^2\left(G'(|\vec{\varkappa}|)\,|\vec{\varkappa}|^{-1}\,\vec{\varkappa}\right) + \left[G(|\vec{\varkappa}|) - G'(|\vec{\varkappa}|)\,|\vec{\varkappa}| + \lambda\right]\vec{\varkappa}$$
$$+ \left(\left[G(|\vec{\varkappa}|)\right]_s - G'(|\vec{\varkappa}|)\left[|\vec{\varkappa}|_s\right]\right)\vec{\tau}$$
$$(2.13)\qquad = -\vec{\nabla}_s^2\left(G'(|\vec{\varkappa}|)\,|\vec{\varkappa}|^{-1}\,\vec{\varkappa}\right) + \left[G(|\vec{\varkappa}|) - G'(|\vec{\varkappa}|)\,|\vec{\varkappa}| + \lambda\right]\vec{\varkappa}.$$

In case (1.3a) with $p = 2$ the above formulas (2.12) and (2.13) collapse to standard elastic flow $\vec{x}_t = -(\vec{\nabla}_s\,\vec{\varkappa})_s - \frac{1}{2}\left(|\vec{\varkappa}|^2\,\vec{\tau}\right)_s + \lambda\,\vec{\varkappa} = -\vec{\nabla}_s^2\,\vec{\varkappa} - \frac{1}{2}\,|\vec{\varkappa}|^2\,\vec{\varkappa} + \lambda\,\vec{\varkappa}$; see also [2, eq. (2.25)]. As the right-hand side in (2.13) is normal to the curve, an alternative formulation of (2.12) is given by

$$(2.14)\qquad \underline{P}\,\vec{x}_t = -\left(\underline{P}\left[G'(|\vec{\varkappa}|)\,|\vec{\varkappa}|^{-1}\,\vec{\varkappa}\right]_s\right)_s + \left(\left[G(|\vec{\varkappa}|) - G'(|\vec{\varkappa}|)\,|\vec{\varkappa}| + \lambda\right]\vec{\tau}\right)_s.$$

3. Weak formulations. We define the first variation of a quantity A depending on $\vec{x}$, in the direction $\vec{\chi}$ as

$$(3.1)\qquad \left[\frac{\delta}{\delta\vec{x}}\,A(\vec{x})\right](\vec{\chi}) = \lim_{\varepsilon\to 0}\frac{A(\vec{x} + \varepsilon\,\vec{\chi}) - A(\vec{x})}{\varepsilon}.$$

For later use, on noting (3.1) and (2.2), we observe that

$$(3.2a)\qquad \left[\frac{\delta}{\delta\vec{x}}\,|\vec{x}_\rho|\right](\vec{\chi}) = \frac{\vec{x}_\rho\cdot\vec{\chi}_\rho}{|\vec{x}_\rho|} = \vec{\tau}\cdot\vec{\chi}_\rho,$$

$$(3.2b)\qquad \left[\frac{\delta}{\delta\vec{x}}\,\vec{\tau}\right](\vec{\chi}) = \left[\frac{\delta}{\delta\vec{x}}\,\frac{\vec{x}_\rho}{|\vec{x}_\rho|}\right](\vec{\chi}) = \frac{1}{|\vec{x}_\rho|}\,\underline{\underline{P}}\,\vec{\chi}_\rho = \underline{P}\,\vec{\chi}_s,$$

$$(3.2c)\qquad \left[\frac{\delta}{\delta\vec{x}}\,\vec{x}_\rho\right](\vec{\chi}) = \vec{\chi}_\rho,$$

where we always assume that $\vec{\chi}$ is sufficiently smooth so that all the quantities are defined almost everywhere; e.g., $\vec{\chi}\in[W^{1,\infty}(I)]^d$. In addition, we note that

$$(3.3)\qquad \left[\frac{\delta}{\delta\vec{x}}\,A(\vec{x})\right](\vec{x}_t) = \frac{d}{dt}\,A(\vec{x}).$$

For example, (2.11) can be read as $[\delta/\delta\vec{x}\,E_\lambda(\vec{x})](\vec{x}_t)$.

3.1. Weak formulation without tangential motion. The differential equations obtained in the previous section are first order in time but fourth order in space. It is in view of numerical methods more convenient to write the equations in $\vec{x}$ and $\vec{\varkappa}$, but coupled by (2.4), since it allows to use first order methods. The weak formulation will then be derived from the corresponding Lagrange function. For convenience we will denote by $(\cdot,\cdot)$ the L^2-inner product on I.

Weak formulation. Given $\Gamma(0) = \vec{x}(I, 0)$, with $\vec{x}(0)\in\underline{V}$ for all $t\in(0, T]$, find $\Gamma(t) = \vec{x}(I, t)$, where $\vec{x}_t(t)\in\underline{W}$, $\vec{\varkappa}(t)\in\underline{V}$ and $\vec{y}(t)\in\underline{V}$, such that

$$(3.4a)\qquad \left(\vec{x}_t, \vec{\chi}\,|\vec{x}_\rho|\right) - \left(\underline{P}\,\vec{y}_s, \vec{\chi}_\rho\right) + \left(G(|\vec{\varkappa}|) + \lambda - \vec{\varkappa}\cdot\vec{y}, \vec{\chi}_\rho\cdot\vec{\tau}\right) = 0\qquad \forall\,\vec{\chi}\in\underline{W}.$$

$$(3.4b)\qquad \left(G'(|\vec{\varkappa}|)\,|\vec{\varkappa}|^{-1}\,\vec{\varkappa} - \vec{y}, \vec{\xi}\,|\vec{x}_\rho|\right) = 0\qquad \forall\,\vec{\xi}\in[L^2(I)]^d,$$

$$(3.4c)\qquad \left(\vec{\varkappa}, \vec{\eta}\,|\vec{x}_\rho|\right) + (\vec{\tau}, \vec{\eta}_\rho) = \sum_{q\in\partial I}\vec{\zeta}_q\cdot\vec{\eta}(q)\qquad \forall\,\vec{\eta}\in\underline{V}.$$

Lagrange formalism. We derive the weak equations by using the formal calculus of PDE constrained optimization; see, e.g., [27]. For our constrained problem we define the Lagrangian

$$\mathcal{L}_1(\vec{x}, \vec{\varkappa}, \vec{y}) = \big(G(|\vec{\varkappa}|) + \lambda, |\vec{x}_\rho|\big) - (\vec{\varkappa}, \vec{y}\,|\vec{x}_\rho|) - (\vec{\tau}, \vec{y}_\rho) + \sum_{q \in \partial I} \vec{\zeta}_q \cdot \vec{y}(q);$$

i.e., we consider the gradient flow of (2.5) subject to the constraint (2.9). Taking variations $\vec{\chi} \in \underline{W}$ in $\vec{x}$ and setting $(\vec{x}_t, \vec{\chi}\,|\vec{x}_\rho|) + \big[\frac{\delta}{\delta \vec{x}} \mathcal{L}_1\big](\vec{\chi}) = 0$, we obtain that

(3.5)

$$(\vec{x}_t, \vec{\chi}\,|\vec{x}_\rho|) + \left(G(|\vec{\varkappa}|) + \lambda - \vec{\varkappa} \cdot \vec{y}, \left[\frac{\delta}{\delta \vec{x}}\,|\vec{x}_\rho|\right](\vec{\chi})\right) - \left(\vec{y}_\rho, \left[\frac{\delta}{\delta \vec{x}}\,\vec{\tau}\right](\vec{\chi})\right) = 0 \quad \forall\ \vec{\chi} \in \underline{W}\,.$$

On recalling (3.2a,b), it follows from (3.5) that

$$\big(\vec{x}_t, \vec{\chi}\,|\vec{x}_\rho|\big) - \big(\underline{P}\,\vec{y}_s, \vec{\chi}_\rho\big) + \big(G(|\vec{\varkappa}|) + \lambda - \vec{\varkappa} \cdot \vec{y}, \vec{\chi}_\rho \cdot \vec{\tau}\big) = 0 \qquad \forall\ \vec{\chi} \in \underline{W}$$

and thus (3.4a). Taking now variations $[\frac{\delta}{\delta \vec{\varkappa}} \mathcal{L}_1](\vec{\xi})$ and $[\frac{\delta}{\delta \vec{y}} \mathcal{L}_1](\vec{\eta})$, for $\vec{\xi} \in [L^2(I)]^d$ and $\vec{\eta} \in \underline{V}$, and setting them to zero yields (3.4b) and (3.4c).

Stability. It follows from (3.4b) that $\vec{y} = G'(|\vec{\varkappa}|)\,|\vec{\varkappa}|^{-1}\,\vec{\varkappa}$, and so the weak form (3.4) reduces to

(3.6a)
$$\big(\vec{x}_t, \vec{\chi}\,|\vec{x}_\rho|\big) - \big(\underline{P}\,[G'(|\vec{\varkappa}|)\,|\vec{\varkappa}|^{-1}\,\vec{\varkappa}]_s, \vec{\chi}_\rho\big)$$
$$+ \big([G(|\vec{\varkappa}|) - G'(|\vec{\varkappa}|)\,|\vec{\varkappa}| + \lambda]\,\vec{\tau}, \vec{\chi}_\rho\big) = 0\,,$$

(3.6b)
$$\big(\vec{\varkappa}, \vec{\eta}\,|\vec{x}_\rho|\big) + \big(\vec{\tau}, \vec{\eta}_\rho\big) = \sum_{q \in \partial I} \vec{\zeta}_q \cdot \vec{\eta}(q)$$

for all $\vec{\chi} \in \underline{W}$ and $\vec{\eta} \in \underline{V}$. Choosing $\vec{\chi} = \vec{x}_t \in \underline{W}$ in (3.6a), on recalling (2.11), yields that $\frac{d}{dt} E_\lambda(\vec{x}) + \big(|\vec{x}_t|^2, |\vec{x}_\rho|\big) = 0$ and thus provides the stability result $\frac{d}{dt} E_\lambda(\vec{x}) \leq 0$.

We remark that in an alternative to the Lagrange formalism above, the weak formulation (3.6) can also be obtained directly by testing (2.12) with functions in $\underline{W}$ and using (2.9). We note that in case (1.3a) with $p = 2$, (3.6) collapses to the weak formulation of [9, eqs. (2.2), (2.3)] for elastic flow.

3.2. Weak formulation with tangential motion. In the following, based on the techniques in [4], we will introduce an alternative weak formulation for the L^2-gradient flow of the energy (2.5), by imposing the two constraints

(3.7a)
$$(\vec{\varkappa}, \vec{\eta}\,|\vec{x}_\rho|) + (\vec{\tau}, \vec{\eta}_\rho) = \sum_{q \in \partial I} \vec{\zeta}_q \cdot \vec{\eta}(q) \qquad \forall\ \vec{\eta} \in \underline{V}$$

(3.7b)   and $$(\vec{\varkappa} \cdot \vec{\tau}, \chi\,|\vec{x}_\rho|) = 0 \qquad\qquad \forall\ \chi \in L^2(I)\,.$$

We recall that the right-hand side in (3.7a) is zero in the case $I = \mathbb{R}/\mathbb{Z}$. Here we should stress that the finite element discretization of the constraints (3.7), building on the ideas published in [4], will lead to an induced tangential motion that gives rise to an equidistribution property in the semidiscrete setting (section 4). Of course, on the continuous level the constraint (3.7b) is redundant, recall (2.4) and (2.1). We will formally establish that solutions to this weak formulation are indeed solutions to the L^2-gradient flow of (2.5). Mimicking this stability proof on the discrete level will yield the main result (Theorem 4.2) of this paper.

Weak formulation. Given $\Gamma(0) = \vec{x}(I,0)$, with $\vec{x}(0) \in \underline{V}$, for all $t \in (0,T]$ find $\Gamma(t) = \vec{x}(I,t)$, where $\vec{x}_t(t) \in \underline{W}$, $\vec{\varkappa}(t) \in \underline{V}$ and $\vec{y}(t) \in \underline{V}$ such that

$$\left(\underline{P}\,\vec{x}_t, \vec{\chi}\,|\vec{x}_\rho|\right) - \left(\underline{P}\,\vec{y}_s, \vec{\chi}_\rho\right) + \left([G(|\vec{\varkappa}|) + \lambda - \vec{\varkappa}\cdot\vec{y}]\,\vec{\tau} + (\vec{y}\cdot\vec{\tau})\,\vec{\varkappa}, \vec{\chi}_\rho\right) = 0$$

(3.8a) $$\forall\,\vec{\chi} \in \underline{W}\,,$$

(3.8b) $$\left(G'(|\vec{\varkappa}|)\,|\vec{\varkappa}|^{-1}\,\vec{\varkappa} - \underline{P}\,\vec{y}, \vec{\xi}\,|\vec{x}_\rho|\right) = 0 \qquad \forall\,\vec{\xi} \in [L^2(I)]^d\,,$$

(3.8c) $$\left(\vec{\varkappa}, \vec{\eta}\,|\vec{x}_\rho|\right) + \left(\vec{\tau}, \vec{\eta}_\rho\right) = \sum_{q\in\partial I} \vec{\zeta}_q \cdot \vec{\eta}(q) \qquad \forall\,\vec{\eta} \in \underline{V}\,.$$

We observe that in the case (1.3a) with $p = 2$, the formulation (3.8), for $I = \mathbb{R}/\mathbb{Z}$, collapses to [4, eq. (2.4)] on noting that then (3.8b) implies that $\vec{\varkappa} = \underline{P}\,\vec{y}$. It is straightforward to show that sufficiently smooth solutions to (3.8) satisfy (2.14), i.e., that the weak formulation (3.8) is consistent with (2.14).

Lagrange formalism. We introduce Lagrange multipliers $\vec{y} \in \underline{V}$ and $z \in L^2(I)$ for (3.7) and define the Lagrangian

$$\mathcal{L}_2(\vec{x}, \vec{\varkappa}, \vec{y}, z) = (G(|\vec{\varkappa}|) + \lambda, |\vec{x}_\rho|) - (\vec{\varkappa}, \vec{y}\,|\vec{x}_\rho|) - (\vec{\tau}, \vec{y}_\rho) + \sum_{q\in\partial I} \vec{\zeta}_q \cdot \vec{y}(q) + (\vec{\varkappa}\cdot\vec{x}_\rho, z)\,.$$

We start by taking variations $[\frac{\delta}{\delta\vec{y}}\mathcal{L}_2](\vec{\eta})$, $[\frac{\delta}{\delta\vec{\varkappa}}\mathcal{L}_2](\vec{\xi})$, $[\frac{\delta}{\delta z}\mathcal{L}_2](\chi)$ and setting them to zero. While the first term immediately yields (3.8c), the remaining equations are

(3.9a) $$\left(G'(|\vec{\varkappa}|)\,|\vec{\varkappa}|^{-1}\,\vec{\varkappa} - \vec{y} + z\,\vec{\tau}, \vec{\xi}\,|\vec{x}_\rho|\right) = 0 \qquad \forall\,\vec{\xi} \in [L^2(I)]^d\,,$$

(3.9b) $$\left(\vec{\varkappa}\cdot\vec{x}_\rho, \chi\right) = 0 \qquad \forall\,\chi \in L^2(I)\,.$$

Taking variations $\vec{\chi} \in \underline{W}$ in $\vec{x}$ and setting $(\underline{P}\,\vec{x}_t, \vec{\chi}\,|\vec{x}_\rho|) + [\frac{\delta}{\delta\vec{x}}\mathcal{L}_2](\vec{\chi}) = 0$ yields that

$$\left(\underline{P}\,\vec{x}_t, \vec{\chi}\,|\vec{x}_\rho|\right) + \left(G(|\vec{\varkappa}|) + \lambda - \vec{\varkappa}\cdot\vec{y}, \left[\frac{\delta}{\delta\vec{x}}|\vec{x}_\rho|\right](\vec{\chi})\right)$$

(3.10) $$- \left(\vec{y}_\rho, \left[\frac{\delta}{\delta\vec{x}}\vec{\tau}\right](\vec{\chi})\right) + \left(z\,\vec{\varkappa}, \left[\frac{\delta}{\delta\vec{x}}\vec{x}_\rho\right](\vec{\chi})\right) = 0 \qquad \forall\,\vec{\chi} \in \underline{W}\,.$$

On recalling (3.2), it follows from (3.10) that

(3.11)
$$\left(\underline{P}\,\vec{x}_t, \vec{\chi}\,|\vec{x}_\rho|\right) + \left(G(|\vec{\varkappa}|) + \lambda - \vec{\varkappa}\cdot\vec{y}, \vec{\tau}\cdot\vec{\chi}_\rho\right) - \left(\vec{y}_\rho, \underline{P}\,\vec{\chi}_s\right) + \left(z\,\vec{\varkappa}, \vec{\chi}_\rho\right) = 0 \quad \forall\,\vec{\chi} \in \underline{W}\,.$$

In addition, it follows from (3.9a,b) by considering the normal and tangential part that $\underline{P}\,\vec{y} = G'(|\vec{\varkappa}|)\,|\vec{\varkappa}|^{-1}\,\vec{\varkappa}$ and $z = \vec{y}\cdot\vec{\tau}$. With the first term we can provide (3.8b), while inserting the second identity into (3.11) gives (3.8a).

Stability. Choosing $\vec{\chi} = \vec{x}_t \in \underline{W}$ in (3.10) and noting (3.3) yields that

(3.12) $$\left(|\underline{P}\,\vec{x}_t|^2, |\vec{x}_\rho|\right) + (G(|\vec{\varkappa}|) + \lambda - \vec{\varkappa}\cdot\vec{y}, (|\vec{x}_\rho|)_t) - (\vec{y}_\rho, \vec{\tau}_t) + (z\,\vec{\varkappa}, \vec{x}_{\rho,t}) = 0\,.$$

Differentiating (3.8c) with respect to time, and then choosing $\vec{\eta} = \vec{y}$ yields

(3.13) $$(\vec{\varkappa}_t, \vec{y}\,|\vec{x}_\rho|) + (\vec{\varkappa}\cdot\vec{y}, (|\vec{x}_\rho|)_t) + (\vec{y}_\rho, \vec{\tau}_t) = 0\,.$$

Differentiating (3.7b) with respect to t, and then choosing $\chi = z$ yields that

(3.14) $$(z\,\vec{\varkappa}_t, \vec{x}_\rho) + (z\,\vec{\varkappa}, \vec{x}_{t,\rho}) = 0\,.$$

Choosing $\vec{\zeta} = \vec{\varkappa}_t$ in (3.9a) yields that

$$(3.15) \qquad (\vec{y} - z\,\vec{\tau}, \vec{\varkappa}_t\,|\vec{x}_\rho|) = \left(G'(|\vec{\varkappa}|)\,|\vec{\varkappa}|^{-1}\,\vec{\varkappa}, \vec{\varkappa}_t\,|\vec{x}_\rho|\right) = \left([G(|\vec{\varkappa}|)]_t\,, |\vec{x}_\rho|\right).$$

Combining (3.12), (3.13), (3.14), and (3.15) yields that

$$
\begin{aligned}
\frac{\mathrm{d}}{\mathrm{d}t}\,E_\lambda(\vec{x}, \vec{\varkappa}) &= \frac{\mathrm{d}}{\mathrm{d}t}\,(G(|\vec{\varkappa}|), |\vec{x}_\rho|) + (\lambda, (|\vec{x}_\rho|)_t) \\
&= ([G(|\vec{\varkappa}|)]_t\,, |\vec{x}_\rho|) + (G(|\vec{\varkappa}|) + \lambda, (|\vec{x}_\rho|)_t) \\
&= (\vec{y} - z\,\vec{\tau}, \vec{\varkappa}_t\,|\vec{x}_\rho|) + (G(|\vec{\varkappa}|) + \lambda, (|\vec{x}_\rho|)_t) \\
&= (G(|\vec{\varkappa}|) + \lambda - \vec{\varkappa}\cdot\vec{y}, (|\vec{x}_\rho|)_t) - (\vec{y}_\rho, \vec{\tau}_t) + (z\,\vec{\varkappa}, \vec{x}_{t,\rho}) \\
&= -\left(|\underline{\underline{P}}\,\vec{x}_t|^2, |\vec{x}_\rho|\right) \le 0,
\end{aligned}
$$

which shows that (3.8) is indeed a weak formulation of the L^2-gradient flow of (2.5).

4. Semidiscrete in space finite element approximation. Let $[0,1] = \cup_{j=1}^J I_j$, $J \ge 3$, be a decomposition of $[0,1]$ into intervals $I_j = [q_{j-1}, q_j]$ given by a set of nodes q_j. For simplicity, and without loss of generality, we assume that the subintervals form an equipartitioning of $[0,1]$, i.e., that

$$(4.1) \qquad q_j = j\,h, \quad \text{with} \quad h = J^{-1}, \qquad j = 0, \ldots, J.$$

In case $I = \mathbb{R}/\mathbb{Z}$ we identify $0 = q_0 = q_J = 1$ and set $q_{J+1} = q_1$.

The finite element spaces we use are given as follows:

$$V^h = \{\chi \in C(\overline{I}) : \chi|_{I_j} \text{ is linear } \forall\, j = 1, \ldots, J\} \quad \text{and} \quad \underline{V}^h = [V^h]^d.$$

Let $\{\chi_j\}_{j=j_0}^J$ denote the standard basis of V^h, where $j_0 = 0$ if $I = (0,1)$ and $j_0 = 1$ if $I = \mathbb{R}/\mathbb{Z}$. We also set $j_1 = J - 1$ if $I = (0,1)$ and $j_1 = J$ if $I = \mathbb{R}/\mathbb{Z}$. Let $\pi^h : C(\overline{I}) \to V^h$ be the standard interpolation operator at the nodes $\{q_j\}_{j=0}^J$, and similarly for $\vec{\pi}^h : [C(I)]^d \to \underline{V}^h$. Moreover, we define the spaces

$$W^h = V^h \cap H_0^1(I) \quad \text{and} \quad \underline{W}^h = [W^h]^d.$$

Let $\pi_W^h : C(\overline{I}) \to W^h$ be the standard Lagrange interpolation operator with zero Dirichlet boundary conditions.

Similarly to $(\cdot, \cdot)$, the L^2-inner product on I, we define the mass-lumped L^2-inner product $(\cdot, \cdot)^h$, for two piecewise continuous functions u, v, with possible jumps at the nodes $\{q_j\}_{j=1}^{J-1}$, via

$$(4.2) \qquad (u, v)^h = \tfrac{1}{2}\,h \sum_{j=1}^J \left[(u\,v)(q_j^-) + (u\,v)(q_{j-1}^+)\right],$$

where we define $u(q_j^\pm) = \lim_{\delta \searrow 0} u(q_j \pm \delta)$. The definition (4.2) naturally extends to vector valued functions.

Let $\vec{X}^h : [0, T] \to \underline{V}^h$ be an approximation to $\vec{x} : [0, T] \to \underline{V}$. Here we make the quite natural assumption that

$(\mathcal{C}_1^h)$ $\vec{X}^h(q_j, t) \ne \vec{X}^h(q_{j+1}, t), \quad j = 0, \ldots, J - 1 \quad \forall\, t \in [0, T].$

Then, in correspondence to (2.2) and (2.8), we set

$$(4.3) \qquad \vec{\tau}^h = \vec{X}_s^h = \frac{\vec{X}_\rho^h}{|\vec{X}_\rho^h|} \quad \text{and} \quad \underline{\underline{P}}^h = \underline{\underline{\text{Id}}} - \vec{\tau}^h \otimes \vec{\tau}^h \,.$$

Moreover, in analogy to (3.2), on noting (3.1) and (4.3), we have for all $\vec{\chi} \in \underline{V}^h$ on I_j, $j = 1, \ldots, J$, that

$$(4.4a) \qquad \left[\frac{\delta}{\delta \vec{X}^h} \, |\vec{X}_\rho^h| \right] (\vec{\chi}) = \frac{\vec{X}_\rho^h \cdot \vec{\chi}_\rho}{|\vec{X}_\rho^h|} = \vec{\tau}^h \cdot \vec{\chi}_\rho \,,$$

$$(4.4b) \qquad \left[\frac{\delta}{\delta \vec{X}^h} \, \vec{\tau}^h \right] (\vec{\chi}) = \left[\frac{\delta}{\delta \vec{X}^h} \, \frac{\vec{X}_\rho^h}{|\vec{X}_\rho^h|} \right] (\vec{\chi}) = \frac{1}{|\vec{X}_\rho^h|} \, \underline{\underline{P}}^h \, \vec{\chi}_\rho = \underline{\underline{P}}^h \, \vec{\chi}_s \,,$$

$$(4.4c) \qquad \left[\frac{\delta}{\delta \vec{X}^h} \, \vec{X}_\rho^h \right] (\vec{\chi}) = \vec{\chi}_\rho \,.$$

Given $\vec{X}^h, \vec{\kappa}^h \in \underline{V}^h$, we define the discrete energy

$$(4.5) \qquad E_\lambda^h(\vec{X}^h, \vec{\kappa}^h) = \left(G(|\vec{\kappa}^h|) + \lambda, |\vec{X}_\rho^h| \right)^h \,.$$

4.1. Semidiscrete method without tangential motion. We consider the following semidiscrete continuous-in-time finite element approximation of (3.4).

Semidiscrete weak formulation. Let $\vec{X}^h(0) \in \underline{V}^h$. For $t \in (0, T]$ find $\vec{X}^h(t)$, $\vec{\kappa}^h(t)$, $\vec{Y}^h(t) \in \underline{V}^h$, with $\vec{X}_t^h(t) \in \underline{W}^h$, such that

$$\left(\vec{X}_t^h, \vec{\chi} \, |\vec{X}_\rho^h| \right)^h - \left(\underline{\underline{P}}^h \, \vec{Y}_s^h, \vec{\chi}_s \, |\vec{X}_\rho^h| \right)$$

$$(4.6a) \qquad + \left([G(|\vec{\kappa}^h|) + \lambda - \vec{\kappa}^h \cdot \vec{Y}^h] \, \vec{X}_s^h, \vec{\chi}_s \, |\vec{X}_\rho^h| \right)^h = 0 \qquad \forall \, \vec{\chi} \in \underline{W}^h \,,$$

$$(4.6b) \qquad \left(G'(|\vec{\kappa}^h|) \, |\vec{\kappa}^h|^{-1} \, \vec{\kappa}^h - \vec{Y}^h, \vec{\xi} \, |\vec{X}_\rho^h| \right)^h = 0 \qquad \forall \, \vec{\xi} \in \underline{V}^h \,,$$

$$(4.6c) \qquad \left(\vec{\kappa}^h, \vec{\eta} \, |\vec{X}_\rho^h| \right)^h + \left(\vec{X}_s^h, \vec{\eta}_s \, |\vec{X}_\rho^h| \right) = \sum_{q \in \partial I} \vec{\zeta}_q \cdot \vec{\eta}(q) \qquad \forall \, \vec{\eta} \in \underline{V}^h \,.$$

In case (1.3a) with $p = 2$, it follows from (4.6b) that $\vec{\kappa}^h = \vec{Y}^h$, and so the scheme (4.6), for the case $I = \mathbb{R}/\mathbb{Z}$, collapses to the scheme (2.9), (2.10) in [9] for the elastic flow of closed curves in $\mathbb{R}^d$.

Semidiscrete Lagrange formalism. On recalling (4.5), and with a view to the constraint (4.6c), we define the discrete Lagrangian

$$\mathcal{L}_1^h(\vec{X}^h, \vec{\kappa}^h, \vec{Y}^h) = \left(G(|\vec{\kappa}^h|) + \lambda, |\vec{X}_\rho^h| \right)^h - \left(\vec{\kappa}^h, \vec{Y}^h \, |\vec{X}_\rho^h| \right)^h - \left(\vec{\tau}^h, \vec{Y}_\rho^h \right) + \sum_{q \in \partial I} \vec{\zeta}_q \cdot \vec{Y}^h(q) \,,$$

where $\vec{Y}^h \in \underline{V}^h$ is a Lagrange multiplier for (4.6c). Taking variations $[\frac{\delta}{\delta \vec{\kappa}^h} \mathcal{L}_1^h](\vec{\xi})$ and $[\frac{\delta}{\delta \vec{Y}^h} \mathcal{L}_1^h](\vec{\eta})$, for $\vec{\xi}, \vec{\eta} \in \underline{V}^h$, and setting them to zero yields immediately (4.6b) and (4.6c). Taking variations $\vec{\chi} \in \underline{W}^h$ in $\vec{X}^h$, and setting $(\vec{X}_t^h, \vec{\chi} \, |\vec{X}_\rho^h|)^h + [\frac{\delta}{\delta \vec{x}} \mathcal{L}_1^h](\vec{\chi}) = 0$ we obtain with (4.4a) that

(4.7)
$$\left(\vec{X}_t^h, \vec{\chi} \, |\vec{X}_\rho^h| \right)^h + \left(G(|\vec{\kappa}^h|) + \lambda - \vec{\kappa}^h \cdot \vec{Y}^h, \vec{\tau}^h \cdot \vec{\chi}_\rho \right)^h - \left(\vec{Y}_\rho^h, \underline{\underline{P}}^h \, \vec{\chi}_s \right) = 0 \quad \forall \, \vec{\chi} \in \underline{W}^h \,,$$

which is equivalent to (4.6a).

Stability. Choosing $\vec{\chi} = \vec{X}_t^h \in \underline{W}^h$ in (4.7) and noting (3.3) yields that

$$(4.8) \qquad \left(|\vec{X}_t^h|^2, |\vec{X}_\rho^h|\right)^h + \left(G(|\vec{\kappa}^h|) + \lambda - \vec{\kappa}^h \cdot \vec{Y}^h, (|\vec{X}_\rho^h|)_t\right)^h - \left(\vec{Y}_\rho^h, \vec{\tau}_t^h\right) = 0\,.$$

Differentiating (4.6c) with respect to time and then choosing $\vec{\eta} = \vec{Y}^h$ yields that

$$(4.9) \qquad \left(\vec{\kappa}_t^h, \vec{Y}^h\,|\vec{X}_\rho^h|\right)^h + \left(\vec{\kappa}^h \cdot \vec{Y}^h, (|\vec{X}_\rho^h|)_t\right)^h + \left(\vec{Y}_\rho^h, \vec{\tau}_t^h\right) = 0\,.$$

Choosing $\vec{\zeta} = \vec{\kappa}_t^h$ in (4.6b) yields that

$$(4.10) \qquad \left(\vec{Y}^h, \vec{\kappa}_t^h\,|\vec{X}_\rho^h|\right)^h = \left(G'(|\vec{\kappa}^h|)\,|\vec{\kappa}^h|^{-1}\,\vec{\kappa}^h, \vec{\kappa}_t^h\,|\vec{X}_\rho^h|\right)^h = \left(\left[G(|\vec{\kappa}^h|)\right]_t, |\vec{X}_\rho^h|\right)^h.$$

Combining (4.8), (4.9), and (4.10) yields that

$$\begin{aligned}
\frac{\mathrm{d}}{\mathrm{d}t}\,E_\lambda^h(\vec{X}^h, \vec{\kappa}^h) &= \frac{\mathrm{d}}{\mathrm{d}t}\left(G(|\vec{\kappa}^h|), |\vec{X}_\rho^h|\right)^h + \left(\lambda, (|\vec{X}_\rho^h|)_t\right)^h \\
&= \left(\left[G(|\vec{\kappa}^h|)\right]_t, |\vec{X}_\rho^h|\right)^h + \left(G(|\vec{\kappa}^h|) + \lambda, (|\vec{X}_\rho^h|)_t\right)^h \\
&= -\left(|\vec{X}_t^h|^2, |\vec{X}_\rho^h|\right)^h \le 0\,,
\end{aligned}$$

and so a solution satisfying (4.6) is stable. In fact, we have shown the following result.

THEOREM 4.1. *Let* $G \in C^1(\mathbb{R}_{\ge 0}, \mathbb{R}_{>0})$ *satisfy* (2.6). *Let* $(\vec{X}^h(t), \vec{\kappa}^h(t),$ $\vec{Y}^h(t))_{t \in (0,T]}$ *denote a solution to* (4.6), *with* $(\vec{X}^h(t))_{t \in (0,T]}$ *satisfying* $(\mathcal{C}_1^h)$. *Then it holds that*

$$\frac{\mathrm{d}}{\mathrm{d}t}\,E_\lambda^h(\vec{X}^h, \vec{\kappa}^h) + \left(|\vec{X}_t^h|^2, |\vec{X}_\rho^h|\right)^h = 0\,.$$

4.2. Semidiscrete method with tangential motion. We now derive a semidiscrete formulation for (3.8). For this we need a few more definitions. Here we make the mild assumption that

$(\mathcal{C}_2^h)$ Let $(\mathcal{C}_1^h)$ hold and let $\vec{X}^h(q_{j-1}, t) \ne \vec{X}^h(q_{j+1}, t)$, $j = 1, \ldots, j_1$, for all $t \in [0, T]$.

Let $\vec{\theta}^h \in \underline{V}^h$ be the mass-lumped L^2–projection of $\vec{\tau}^h$ onto $\underline{V}^h$, i.e.,

$$(4.11) \qquad \left(\vec{\theta}^h, \vec{\varphi}\,|\vec{X}_\rho^h|\right)^h = \left(\vec{\tau}^h, \vec{\varphi}\,|\vec{X}_\rho^h|\right) = \left(\vec{\tau}^h, \vec{\varphi}\,|\vec{X}_\rho^h|\right)^h \qquad \forall\,\vec{\varphi} \in \underline{V}^h\,.$$

Following the notation in [4, eq. (3.3)], we then define $\vec{\omega}_d^h(t) \in \underline{V}^h$ to be

$$(4.12) \qquad \vec{\omega}_d^h(t) = \frac{\vec{\theta}^h(t)}{|\vec{\theta}^h(t)|}\,,$$

which, on noting assumption $(\mathcal{C}_2^h)$, is well defined. Let

$$(4.13) \qquad \underline{\underline{Q}}^h(\rho, t) = \underline{\underline{\mathrm{Id}}} - \vec{\omega}_d^h(\rho, t) \otimes \vec{\omega}_d^h(\rho, t) \qquad \forall\,\rho \in [0, 1] \;\; \forall\,t \in [0, T]\,,$$

and introduce the modified operator

$$(4.14) \qquad \underline{\underline{Q}}_\star^h(\rho, t) = \begin{cases} \underline{\underline{Q}}^h(\rho, t) & \forall\,\rho \in I\,, \\ \underline{\underline{\mathrm{Id}}} & \forall\,\rho \in \partial I\,. \end{cases}$$

Semidiscrete weak formulation. Let $\vec{X}^h(0) \in \underline{V}^h$. For $t \in (0, T]$ find $\vec{X}^h(t)$, $\vec{\kappa}^h(t)$, $\vec{Y}^h(t) \in \underline{V}^h$, with $\vec{X}^h_t(t) \in \underline{W}^h$, such that

$$\left(\underline{\underline{Q}}^h \, \vec{X}^h_t, \vec{\chi} \, |\vec{X}^h_\rho|\right)^h - \left(\underline{\underline{P}}^h \, \vec{Y}^h_s, \vec{\chi}_s \, |\vec{X}^h_\rho|\right)$$

$$= -\left([G(|\vec{\kappa}^h|) + \lambda - \vec{\kappa}^h \cdot \vec{Y}^h] \, \vec{X}^h_s, \vec{\chi}_s \, |\vec{X}^h_\rho|\right)^h$$

(4.15a)
$$- \left(\pi^h_W \, [|\vec{\theta}^h|^{-1} \, (\vec{Y}^h \cdot \vec{\omega}^h_d)] \, \vec{\kappa}^h, \vec{\chi}_s \, |\vec{X}^h_\rho|\right)^h \qquad \forall \, \vec{\chi} \in \underline{W}^h \,,$$

(4.15b)
$$\left(G'(|\vec{\kappa}^h|) \, |\vec{\kappa}^h|^{-1} \, \vec{\kappa}^h - \underline{\underline{Q}}^h_\star \, \vec{Y}^h, \vec{\xi} \, |\vec{X}^h_\rho|\right)^h = 0 \qquad \forall \, \vec{\xi} \in \underline{V}^h \,,$$

(4.15c)
$$\left(\vec{\kappa}^h, \vec{\eta} \, |\vec{X}^h_\rho|\right)^h + \left(\vec{X}^h_s, \vec{\eta}_s \, |\vec{X}^h_\rho|\right) = \sum_{q \in \partial I} \vec{\zeta}_q \cdot \vec{\eta}(q) \qquad \forall \, \vec{\eta} \in \underline{V}^h \,.$$

Discrete Lagrangian. We consider the L^2-gradient flow of the discrete energy (4.5), subject to the constraints

(4.16a)
$$\left(\vec{\kappa}^h, \vec{\eta} \, |\vec{X}^h_\rho|\right)^h + \left(\vec{X}^h_s, \vec{\eta}_s \, |\vec{X}^h_\rho|\right) = \sum_{q \in \partial I} \vec{\zeta}_q \cdot \vec{\eta}(q) \qquad \forall \, \vec{\eta} \in \underline{V}^h$$

(4.16b)   and
$$\left(\vec{\kappa}^h \cdot \vec{X}^h_\rho, \chi\right)^h = 0 \qquad \forall \, \chi \in W^h \,.$$

To this end, we define the discrete Lagrangian

$$\mathcal{L}^h_2(\vec{X}^h, \vec{\kappa}^h, \vec{Y}^h, Z^h) = \left(G(|\vec{\kappa}^h|) + \lambda, |\vec{X}^h_\rho|\right)^h - \left(\vec{\kappa}^h, \vec{Y}^h |\vec{X}^h_\rho|\right)^h - \left(\vec{\tau}^h, \vec{Y}^h_\rho\right)$$

$$+ \sum_{q \in \partial I} \vec{\zeta}_q \cdot \vec{Y}^h(q) + \left(\vec{\kappa}^h \cdot \vec{X}^h_\rho, Z^h\right)^h \,,$$

where $\vec{Y}^h \in \underline{V}^h$ and $Z^h \in W^h$ are Lagrange multipliers for (4.16a) and (4.16b), respectively. Here the test space W^h in (4.16b) was chosen because it is sufficient to obtain the desired equidistribution result, and this leads to the altered projection $\underline{\underline{Q}}^h_\star$ in (4.15b). For the choice (1.3a) with $p = 2$, the same strategy was employed in [4].

We take variations $[\frac{\delta}{\delta \vec{Y}^h} \mathcal{L}^h_2](\vec{\eta})$, $[\frac{\delta}{\delta \vec{\kappa}^h} \mathcal{L}^h_2](\vec{\xi})$, and $[\frac{\delta}{\delta Z^h} \mathcal{L}^h_2](\chi)$, for $\vec{\xi}, \vec{\eta} \in \underline{V}^h$, $\chi \in W^h$, and set them to zero. This yields (4.15c),

(4.17)
$$\left(G'(|\vec{\kappa}^h|) \, |\vec{\kappa}^h|^{-1} \, \vec{\kappa}^h - \vec{Y}^h + Z^h \, \vec{\tau}^h, \vec{\xi} \, |\vec{X}^h_\rho|\right)^h = 0 \qquad \forall \, \vec{\xi} \in \underline{V}^h$$

and (4.16b).

Taking variations $\vec{\chi} \in \underline{W}^h$ in $\vec{X}^h$ and setting $(\underline{\underline{Q}}^h \, \vec{X}^h_t, \vec{\chi} \, |\vec{X}^h_\rho|)^h + \left[\frac{\delta}{\delta \vec{x}} \mathcal{L}^h_2\right](\vec{\chi}) = 0$ we obtain that

$$\left(\underline{\underline{Q}}^h \, \vec{X}^h_t, \vec{\chi} \, |\vec{X}^h_\rho|\right)^h + \left(G(|\vec{\kappa}^h|) + \lambda - \vec{\kappa}^h \cdot \vec{Y}^h, \left[\frac{\delta}{\delta \vec{X}^h} \, |\vec{X}^h_\rho|\right](\vec{\chi})\right)^h$$

(4.18)
$$- \left(\vec{Y}^h_\rho, \left[\frac{\delta}{\delta \vec{X}^h} \, \vec{\tau}^h\right](\vec{\chi})\right) + \left(Z^h \, \vec{\kappa}^h, \left[\frac{\delta}{\delta \vec{X}^h} \, \vec{X}^h_\rho\right](\vec{\chi})\right)^h = 0 \qquad \forall \, \vec{\chi} \in \underline{W}^h \,.$$

On recalling (4.4), it follows from (4.18) that

$$\left(\underline{\underline{Q}}^h \, \vec{X}^h_t, \vec{\chi} \, |\vec{X}^h_\rho|\right)^h + \left(G(|\vec{\kappa}^h|) + \lambda - \vec{\kappa}^h \cdot \vec{Y}^h, \vec{\tau}^h \cdot \vec{\chi}_\rho\right)^h - \left(\vec{Y}^h_\rho, \underline{\underline{P}}^h \, \vec{\chi}_s\right)$$

(4.19)
$$+ \left(Z^h \, \vec{\kappa}^h, \vec{\chi}_\rho\right)^h = 0 \qquad \forall \, \vec{\chi} \in \underline{W}^h \,.$$

It remains to identify Z^h. It follows from (4.16b) and (4.11) (recall also (4.2)) that

$$(4.20) \quad 0 = \left(\vec{\kappa}^h \cdot \vec{X}_\rho^h, \chi \right)^h = \left(\vec{\kappa}^h, \chi \, \vec{\tau}^h \, |\vec{X}_\rho^h| \right)^h = \left(\vec{\kappa}^h, \chi \, \vec{\theta}^h \, |\vec{X}_\rho^h| \right)^h \qquad \forall \, \chi \in W^h \,,$$

which together with (4.17) implies that

$$(4.21) \quad 0 = \left(\vec{Y}^h - Z^h \, \vec{\tau}^h, \chi \, \vec{\theta}^h \, |\vec{X}_\rho^h| \right)^h = \left(\vec{Y}^h - Z^h \, \vec{\theta}^h, \chi \, \vec{\theta}^h \, |\vec{X}_\rho^h| \right)^h \qquad \forall \, \chi \in W^h \,.$$

As $Z^h \in W^h$ this shows, on recalling (4.2) and (4.12), that

$$(4.22) \qquad\qquad Z^h = \pi_W^h \left[|\vec{\theta}^h|^{-2} \, \vec{Y}^h \cdot \vec{\theta}^h \right] = \pi_W^h \left[|\vec{\theta}^h|^{-1} \, \vec{Y}^h \cdot \vec{\omega}_d^h \right] \,.$$

Combining (4.22) with (4.17) yields that $\vec{\pi}^h \, [\underline{\underline{Q_\star^h}} \, \vec{Y}^h] = \vec{\pi}^h \, [G'(|\vec{\kappa}^h|) \, |\vec{\kappa}^h|^{-1} \, \vec{\kappa}^h]$. This gives (4.15b) and inserting Z^h in (4.19) yields (4.15a).

Stability. Choosing $\vec{\chi} = \vec{X}_t^h \in \underline{W}^h$ in (4.18) and noting (3.3) yields that

$$\left(|\underline{\underline{Q}}^h \, \vec{X}_t^h|^2, |\vec{X}_\rho^h| \right)^h + \left(G(|\vec{\kappa}^h|) + \lambda - \vec{\kappa}^h \cdot \vec{Y}^h, (|\vec{X}_\rho^h|)_t \right)^h - \left(\vec{Y}_\rho^h, \vec{\tau}_t^h \right)$$

$$(4.23) \qquad\qquad\qquad + \left(Z^h \, \vec{\kappa}^h, \vec{X}_{\rho,t}^h \right)^h = 0 \,.$$

Differentiating (4.15c) with respect to time and then choosing $\vec{\eta} = \vec{Y}^h$ yields

$$(4.24) \qquad \left(\vec{\kappa}_t^h, \vec{Y}^h \, |\vec{X}_\rho^h| \right)^h + \left(\vec{\kappa}^h \cdot \vec{Y}^h, (|\vec{X}_\rho^h|)_t \right)^h + \left(\vec{Y}_\rho^h, \vec{\tau}_t^h \right) = 0 \,,$$

i.e., the same as (4.9). Differentiating (4.16b) with respect to t and then choosing $\chi = Z^h$ yields that

$$(4.25) \qquad\qquad \left(Z^h \, \vec{\kappa}_t^h, \vec{X}_\rho^h \right)^h + \left(Z^h \, \vec{\kappa}^h, \vec{X}_{t,\rho}^h \right)^h = 0 \,.$$

Choosing $\vec{\zeta} = \vec{\kappa}_t^h$ in (4.17) yields that

$$(4.26)$$
$$\left(\vec{Y}^h - Z^h \, \vec{\tau}^h, \vec{\kappa}_t^h \, |\vec{X}_\rho^h| \right)^h = \left(G'(|\vec{\kappa}^h|) \, |\vec{\kappa}^h|^{-1} \, \vec{\kappa}^h, \vec{\kappa}_t^h \, |\vec{X}_\rho^h| \right)^h = \left([G(|\vec{\kappa}^h|)]_t \,, |\vec{X}_\rho^h| \right)^h \,.$$

Combining (4.23), (4.24), (4.25), and (4.26) yields that

$$\begin{aligned}
\frac{\mathrm{d}}{\mathrm{d}t} E_\lambda^h(\vec{X}^h, \vec{\kappa}^h) &= \frac{\mathrm{d}}{\mathrm{d}t} \left(G(|\vec{\kappa}^h|), |\vec{X}_\rho^h| \right)^h + \left(\lambda, (|\vec{X}_\rho^h|)_t \right)^h \\
&= \left([G(|\vec{\kappa}^h|)]_t \,, |\vec{X}_\rho^h| \right)^h + \left(G(|\vec{\kappa}^h|) + \lambda, (|\vec{X}_\rho^h|)_t \right)^h \\
&= \left(\vec{Y}^h - Z^h \, \vec{\tau}^h, \vec{\kappa}_t^h \, |\vec{X}_\rho^h| \right)^h + \left(G(|\vec{\kappa}^h|) + \lambda, (|\vec{X}_\rho^h|)_t \right)^h \\
&= \left(G(|\vec{\kappa}^h|) + \lambda - \vec{\kappa}^h \cdot \vec{Y}^h, (|\vec{X}_\rho^h|)_t \right)^h - \left(\vec{Y}_\rho^h, \vec{\tau}_t^h \right) + \left(Z^h \, \vec{\kappa}^h, \vec{X}_{t,\rho}^h \right)^h \\
&= - \left(|\underline{\underline{Q}}^h \, \vec{X}_t^h|^2, |\vec{X}_\rho^h| \right)^h \le 0 \,,
\end{aligned}$$

and so a solution satisfying (4.15) is stable.

Equidistribution. Next we show an equidistribution property for the scheme (4.15). Choosing $\vec{\xi} = \vec{\omega}_d^h(q_j)\,\chi_j$ in (4.15b) and $\vec{\eta} = \vec{\omega}_d^h(q_j)\,\chi_j$ in (4.15c), for $j = 1, \ldots, j_1$, yields, on recalling (4.13) and (4.14), that

$$(4.27a) \qquad\qquad G'(|\vec{\kappa}^h(q_j)|)\,|\vec{\kappa}^h(q_j)|^{-1}\,\vec{\kappa}^h(q_j) \cdot \vec{\omega}_d^h(q_j) = 0\,,$$

$$(4.27b) \qquad \vec{\kappa}^h(q_j) \cdot \vec{\omega}_d^h(q_j)\left(\chi_j, |\vec{X}_\rho^h|\right) + \left(\vec{X}_s^h, (\vec{\omega}_d^h(q_j)\,\chi_j)_\rho\right) = 0\,.$$

It follows from (4.27b), on setting $\vec{a}_{j-\frac{1}{2}}^h = \vec{X}(q_j) - \vec{X}(q_{j-1})$ and on noting that $\vec{\omega}_d^h(q_j) = \frac{\vec{a}_{j+\frac{1}{2}}^h + \vec{a}_{j-\frac{1}{2}}^h}{|\vec{a}_{j+\frac{1}{2}}^h + \vec{a}_{j-\frac{1}{2}}^h|}$, that

$$(4.28) \qquad \vec{\kappa}^h(q_j) \cdot \vec{\omega}_d^h(q_j)\left(\chi_j, |\vec{X}_\rho^h|\right) + \frac{1}{2}\left(\frac{\vec{a}_{j+\frac{1}{2}}^h}{|\vec{a}_{j+\frac{1}{2}}^h|} - \frac{\vec{a}_{j-\frac{1}{2}}^h}{|\vec{a}_{j-\frac{1}{2}}^h|}\right) \cdot \frac{\vec{a}_{j+\frac{1}{2}}^h + \vec{a}_{j-\frac{1}{2}}^h}{|\vec{a}_{j+\frac{1}{2}}^h + \vec{a}_{j-\frac{1}{2}}^h|} = 0\,.$$

If we assume that $G'(z) \neq 0$ for $z > 0$, then it follows from (4.27a) that $|\vec{\kappa}^h(q_j)| = 0$ or that $\vec{\kappa}^h(q_j) \cdot \vec{\omega}_d^h(q_j) = 0$, i.e., the latter always holds. Hence it follows from (4.28) that

$$\left(\frac{\vec{a}_{j+\frac{1}{2}}^h}{|\vec{a}_{j+\frac{1}{2}}^h|} - \frac{\vec{a}_{j-\frac{1}{2}}^h}{|\vec{a}_{j-\frac{1}{2}}^h|}\right) \cdot \left(\vec{a}_{j+\frac{1}{2}}^h + \vec{a}_{j-\frac{1}{2}}^h\right) = 0\,,$$

which together with the Cauchy–Schwarz inequality implies that $|\vec{a}_{j+\frac{1}{2}}^h| = |\vec{a}_{j-\frac{1}{2}}^h|$ if $\vec{a}_{j+\frac{1}{2}}^h$ is not parallel to $\vec{a}_{j-\frac{1}{2}}^h$.

Overall we have shown the following results.

THEOREM 4.2. *Let* $G \in C^1(\mathbb{R}_{\geq 0}, \mathbb{R}_{>0})$ *satisfy* (2.6). *Let* $(\vec{X}^h(t), \vec{\kappa}^h(t), \vec{Y}^h(t))_{t \in (0,T]}$ *denote a solution to* (4.15), *with* $(\vec{X}^h(t))_{t \in (0,T]}$ *satisfying* $(\mathcal{C}_2^h)$. *Then it holds that*

$$\frac{\mathrm{d}}{\mathrm{d}t} E_\lambda^h(\vec{X}^h, \vec{\kappa}^h) + \left(|\underline{\underline{Q}}^h\,\vec{X}_t^h|^2, |\vec{X}_\rho^h|\right)^h = 0\,.$$

Moreover, if $G'(z) \neq 0$ *for* $z > 0$, *then on letting* $\vec{a}_{j+\frac{1}{2}}^h = \vec{X}^h(q_j, t) - \vec{X}^h(q_{j+1}, t)$, $j = 0, \ldots, j_1$, *for a fixed time* $t \in (0, T]$, *it holds for* $j = 1, \ldots, j_1$ *that*

$$|\vec{a}_{j+\frac{1}{2}}^h| = |\vec{a}_{j-\frac{1}{2}}^h| \quad \textit{if} \quad \vec{a}_{j+\frac{1}{2}}^h \nparallel \vec{a}_{j-\frac{1}{2}}^h\,.$$

Remark 4.3. We note that the assumption $G'(z) \neq 0$ for $z > 0$ is satisfied for all the choices in (1.3). The proof of the equidistribution properties highlights that a weaker sufficient condition is given by $G'(|\vec{\kappa}^h(q_j)|) \neq 0$, for $j = 1, \ldots, j_1$.

We also stress that the equidistribution property is what sets the approximation (4.15) apart from (4.6), and this is what makes fully discrete variants of the former more practical than fully discrete versions of the latter.

5. Fully discrete finite element approximation. Let $0 = t_0 < t_1 < \cdots < t_{M-1} < t_M = T$ be a partitioning of $[0, T]$ into possibly variable time steps $\Delta t_m = t_{m+1} - t_m$, $m = 0 \to M - 1$. For a given $\vec{X}^m \in \underline{V}^h$ we let $\vec{\tau}^m, \underline{P}^m, \vec{\theta}^m, \vec{\omega}_d^m$ and $\underline{\underline{Q}}_\star^m$ be the natural fully discrete analogues of (4.3), (4.11), (4.12), and (4.14), respectively.

5.1. Fully discrete scheme without tangential motion. On recalling (4.6) we introduce the following fully discrete approximation of (3.4). Given $\vec{X}^0 \in \underline{V}^h$ with $\vec{X}^0(q) = \vec{\alpha}_q$ for $q \in \partial I$ and suitably chosen $\vec{\kappa}^0 \in \underline{V}^h$ and $\vec{Y}^0 \in \underline{V}^h$, find $(\delta\vec{X}^{m+1}, \vec{\kappa}^{m+1}, \vec{Y}^{m+1}) \in \underline{W}^h \times \underline{V}^h \times \underline{V}^h$, with $\vec{X}^{m+1} = \vec{X}^m + \delta\vec{X}^{m+1}$, such that for $m = 0, \ldots, M-1$

$$\frac{1}{\Delta t_m} \left(\delta\vec{X}^{m+1}, \vec{\chi} \,|\vec{X}_\rho^m| \right)^h - \left(\underline{\underline{P}}^m \, \vec{Y}_s^{m+1}, \vec{\chi}_s \,|\vec{X}_\rho^m| \right)$$

(5.1a)
$$= -\left([G(|\vec{\kappa}^m|) + \lambda - \vec{\kappa}^m \cdot \vec{Y}^m] \, \vec{X}_s^m, \vec{\chi}_s \,|\vec{X}_\rho^m| \right)^h \qquad \forall\, \vec{\chi} \in \underline{W}^h \,,$$

(5.1b)
$$\left(G'(|\vec{\kappa}^{m+1}|) \,|\vec{\kappa}^{m+1}|^{-1} \, \vec{\kappa}^{m+1} - \vec{Y}^{m+1}, \vec{\xi} \,|\vec{X}_\rho^m| \right)^h = 0 \qquad \forall\, \vec{\xi} \in \underline{V}^h \,,$$

(5.1c)
$$\left(\vec{\kappa}^{m+1}, \vec{\eta} \,|\vec{X}_\rho^m| \right)^h + \left(\vec{X}_s^{m+1}, \vec{\eta}_s \,|\vec{X}_\rho^m| \right) = \sum_{q \in \partial I} \vec{\zeta}_q \cdot \vec{\eta}(q) \qquad \forall\, \vec{\eta} \in \underline{V}^h \,.$$

We observe that in the case (1.3a) with $p = 2$, it follows from (5.1b) that $\vec{\kappa}^{m+1} = \vec{Y}^{m+1}$, and so the scheme (5.1), in the case $I = \mathbb{R}/\mathbb{Z}$, collapses to a fully discrete variant of the scheme (2.9), (2.10) in [9] for elastic flow, compare also with [2, eq. (3.7)].

5.2. Fully discrete scheme with tangential motion. Built on (4.15) we introduce the following fully discrete approximation of (3.8). Given $\vec{X}^0 \in \underline{V}^h$ with $\vec{X}^0(q) = \vec{\alpha}_q$ for $q \in \partial I$ and suitably chosen $\vec{\kappa}^0 \in \underline{V}^h$ and $\vec{Y}^0 \in \underline{V}^h$, find $(\delta\vec{X}^{m+1}, \vec{\kappa}^{m+1}, \vec{Y}^{m+1}) \in \underline{W}^h \times \underline{V}^h \times \underline{V}^h$, with $\vec{X}^{m+1} = \vec{X}^m + \delta\vec{X}^{m+1}$, such that for $m = 0, \ldots, M-1$

$$\frac{1}{\Delta t_m} \left(\underline{\underline{Q}}_\star^m \, \delta\vec{X}^{m+1}, \vec{\chi} \,|\vec{X}_\rho^m| \right)^h - \left(\vec{Y}_s^{m+1}, \vec{\chi}_s \,|\vec{X}_\rho^m| \right)$$

$$+ \left((\vec{\mathrm{Id}} - \underline{\underline{P}}^m) \, \vec{Y}_s^m, \vec{\chi}_s \,|\vec{X}_\rho^m| \right) = -\left([G(|\vec{\kappa}^m|) + \lambda - \vec{\kappa}^m \cdot \vec{Y}^m] \, \vec{X}_s^m, \vec{\chi}_s \,|\vec{X}_\rho^m| \right)^h$$

(5.2a)
$$- \left(\pi_W^h \, [|\vec{\theta}^m|^{-1} \, (\vec{Y}^m \cdot \vec{\omega}_d^m)] \, \vec{\kappa}^m, \vec{\chi}_s \,|\vec{X}_\rho^m| \right)^h \quad \forall\, \vec{\chi} \in \underline{W}^h \,,$$

(5.2b)
$$\left(G'(|\vec{\kappa}^{m+1}|) \,|\vec{\kappa}^{m+1}|^{-1} \, \vec{\kappa}^{m+1} - \underline{\underline{Q}}_\star^m \, \vec{Y}^{m+1}, \vec{\xi} \,|\vec{X}_\rho^m| \right)^h = 0 \quad \forall\, \vec{\xi} \in \underline{V}^h \,,$$

(5.2c)
$$\left(\vec{\kappa}^{m+1}, \vec{\eta} \,|\vec{X}_\rho^m| \right)^h + \left(\vec{X}_s^{m+1}, \vec{\eta}_s \,|\vec{X}_\rho^m| \right) = \sum_{q \in \partial I} \vec{\zeta}_q \cdot \vec{\eta}(q) \quad \forall\, \vec{\eta} \in \underline{V}^h \,.$$

We note that as $\delta\vec{X}^{m+1} \in \underline{W}^h$, it holds that $\underline{\underline{Q}}_\star^m$ in the first term in (5.2a) can be replaced by $\underline{\underline{Q}}^m$.

Remark 5.1.
- We observe that in the case (1.3a) with $p = 2$, it follows from (5.2b) that $\vec{\kappa}^{m+1} = \vec{\pi}^h \,[\underline{\underline{Q}}_\star^m \, \vec{Y}^{m+1}]$, and so our scheme (5.2) collapses to the linear schemes (4.1), if $I = \mathbb{R}/\mathbb{Z}$, and (4.9), if $I = (0, 1)$, in [4]. We recall from [4, Theorems 4.1 and 4.3] that these schemes admit a unique solution, and this is the reason for the chosen time-discretisation of the terms involving $\vec{Y}^{m+1}$ and $\vec{Y}^m$ in (5.2a); see also [4, Remark 4.1].
- For general G, the scheme (5.2) is (mildly) nonlinear and can be solved with the help of a Newton iterative solver. An alternative, linear scheme can be obtained by replacing $G'(|\vec{\kappa}^{m+1}|) \,|\vec{\kappa}^{m+1}|^{-1}$ in (5.2b) with $G'(|\vec{\kappa}^m|) \,|\vec{\kappa}^m|^{-1}$.

However, in practice such a scheme does not perform well, with the scheme breaking down, for example, because $|\vec{\kappa}^{m+1}|$ becomes too small. That is why we prefer the nonlinear scheme (5.2).

- The main difference between the two schemes (5.1) and (5.2) is that the former uses the standard discrete curvature vector $\vec{\kappa}^{m+1}$ as a variable, which leads to mainly normal motion for $\vec{X}^{m+1}$. This is in the spirit of the seminal works by Dziuk; see e.g. [13, 14, 15, 9]. The scheme (5.2), on the other hand, enforces $\vec{\kappa}^{m+1}$ to have no tangential components, which leads to an implicit tangential motion in $\vec{X}^{m+1}$ that gives equidistributed meshes, at least in the semidiscrete limit; recall Theorem 4.2. This is in the spirit of the works by Barrett, Garcke, and Nürnberg; see, e.g., [2, 3, 4] for the case of discrete curve evolutions.

5.3. Solution of the nonlinear system of equations. With the obvious abuse of notation, i.e., on letting $\vec{Y}^{m+1}$, $\delta\vec{X}^{m+1}$, κ^{m+1} also denote the vector of coefficients with respect to the basis functions of $\underline{V}^h$, we can write the nonlinear systems (5.1) and (5.2) as

$$(5.3) \qquad \begin{pmatrix} \underline{\underline{A}} & -\frac{1}{\Delta t_m}\underline{\underline{\mathcal{M}}} & 0 \\ 0 & \underline{\underline{A}} & \underline{M} \\ -\underline{\underline{\mathcal{M}}} & 0 & \underline{\underline{M}}_G(\vec{\kappa}^{m+1}) \end{pmatrix} \begin{pmatrix} \vec{Y}^{m+1} \\ \delta\vec{X}^{m+1} \\ \vec{\kappa}^{m+1} \end{pmatrix} = \begin{pmatrix} \vec{g}^m \\ \vec{f}^m \\ \vec{0} \end{pmatrix},$$

where the definitions of the matrices and vectors in (5.3) follow from (5.1) and (5.2). In particular, for (5.2), and in the case $I = \mathbb{R}/\mathbb{Z}$, the block diagonal matrices $\underline{\underline{\mathcal{M}}}$, $\underline{\underline{M}}_G(\vec{\kappa}^{m+1})$, and $\underline{M}$ are defined by their diagonal block entries

$$\underline{\underline{\mathcal{M}}}_{jj} = M_{jj}\,\underline{\underline{Q}}^m_\star(q_j)\,, \quad [\underline{\underline{M}}_G(\vec{\kappa}^{m+1})]_{jj} = G'(|\vec{\kappa}^{m+1}(q_j)|)\,|\vec{\kappa}^{m+1}(q_j)|^{-1}\,M_{jj}\,\underline{\mathrm{Id}}\,,$$

$$\underline{\underline{M}}_{jj} = M_{jj}\,\underline{\mathrm{Id}}\,, \quad M_{jj} = \left(\chi_j, |\vec{X}^m_\rho|\right), \quad j = j_0, \ldots, J\,.$$

The Jacobian matrix of (5.3) at a Newton iterate $(\vec{Y}^N, \delta\vec{X}^N, \vec{\kappa}^N)^T$ is independent of $\vec{Y}^N, \delta\vec{X}^N$, and can be written as

$$(5.4) \qquad \begin{pmatrix} \underline{\underline{A}} & -\frac{1}{\Delta t_m}\underline{\underline{\mathcal{M}}} & 0 \\ 0 & \underline{\underline{A}} & \underline{M} \\ -\underline{\underline{\mathcal{M}}} & 0 & \underline{\underline{M}}_{dG}(\vec{\kappa}^N) \end{pmatrix},$$

where

$$[\underline{\underline{M}}_{dG}(\vec{\kappa}^N)]_{jj} = M_{jj}\left(G'(|\vec{\kappa}^N(q_j)|)\,|\vec{\kappa}^N(q_j)|^{-1}\,\underline{\mathrm{Id}}\right.$$
$$\left. + \left[G''(|\vec{\kappa}^N(q_j)|) - G'(|\vec{\kappa}^N(q_j)|)\,|\vec{\kappa}^N(q_j)|^{-1}\right]|\vec{\kappa}^N(q_j)|^{-2}\,\vec{\kappa}^N(q_j)\otimes\vec{\kappa}^N(q_j)\right).$$

We note that for the cases (1.3a)–(1.3c) we have

$$(5.5a) \quad G'(z)/z = z^{p-2}\,, \qquad\qquad G''(z) = (p-1)\,z^{p-2}\,,$$

$$(5.5b) \quad G'(z)/z = \alpha\,z^{-3}\,e^{-\alpha/z}\,, \qquad\qquad G''(z) = \alpha\,(\alpha - 2\,z)\,z^{-4}\,e^{-\alpha/z}\,,$$

$$(5.5c) \quad G'(z)/z = \tfrac{1}{2}\,z^{-\frac{5}{2}}\,(z + 2\,\alpha)\,e^{-\alpha/z}\,, \quad G''(z) = \tfrac{1}{4}\,z^{-\frac{7}{2}}\,(z^2 + 4\,\alpha\,z - 4\,\alpha^2)\,e^{-\alpha/z}\,.$$

In practice the Newton iteration for (5.3), for the schemes (5.1) and (5.2), usually converges in only a few steps. We implemented the schemes (5.1) and (5.2) with the help of the finite element toolbox ALBERTA; see [26]. The linear subproblems of the Newton iteration, featuring the block matrix (5.4), are solved with the help of the sparse factorization package UMFPACK; see [8].

6. Numerical results. Throughout the numerical experiments we take, for given $\vec{X}_0$, $\vec{\kappa}^0 = \underline{\underline{Q}}^0 \, \vec{k}$, where $\vec{k} \in \underline{V}^h$ is the solution to

$$\left(\vec{k}, \vec{\eta} \, |\vec{X}_\rho^0|\right)^h + \left(\vec{X}_s^0, \vec{\eta}_s \, |\vec{X}_\rho^0|\right) = \sum_{q \in \partial I} \vec{\zeta}_q \cdot \vec{\eta}(q) \qquad \forall \, \vec{\eta} \in \underline{V}^h \, ,$$

and then set $\vec{Y}^0 = \vec{\pi}^h \, [G'(|\vec{\kappa}^0|) \, |\vec{\kappa}^0|^{-1} \, \vec{\kappa}^0]$. We will always employ uniform time steps, $\Delta t_m = \Delta t$, $m = 0, \ldots, M - 1$. For the spatial resolution we will refer to h_{Γ^0}, the maximal edge length of Γ^0. On recalling (4.5), we will refer to $E_\lambda^h(\vec{X}^m, \vec{\kappa}^{m+1})$ as the fully discrete energy for solutions of the schemes (5.1) and (5.2), respectively. We stress that no remeshing was used in any of the experiments presented in this section.

6.1. Numerical results for $d = 2$.

6.1.1. Circular solutions. For the choice (1.3a), we recall the true solution (A.3) with (A.5) for (2.12) with $\lambda = 0$ from the appendix. It will be used for the convergence tests for the presented schemes. To this end, we start with the initial data

$$(6.1) \qquad \vec{X}^0(q_j) = r(0) \begin{pmatrix} \cos[2 \, \pi \, q_j + 0.1 \, \sin(2 \, \pi \, q_j)] \\ \sin[2 \, \pi \, q_j + 0.1 \, \sin(2 \, \pi \, q_j)] \end{pmatrix}, \quad j = 1, \ldots, J \, ;$$

recall (4.1), with $r(0) = 1$. We compute the error

$$(6.2) \qquad \|\Gamma - \Gamma^h\|_{L^\infty} = \max_{m=1,\ldots,M} \max_{j=1,\ldots,J} \left| |\vec{X}^m(q_j)| - r(t_m) \right|$$

over the time interval $[0, 1]$ between the true solution and the discrete solutions. Here we use the time step size $\Delta t = 0.1 \, h_{\Gamma^0}^2$. For the choices $p = 2$, $p = 5$, and $p = 1.1$ the computed errors, together with their experimental order of convergence (EOC), are reported in Tables 1–3. In each case we observe that the schemes exhibit second order convergence rates.

TABLE 1
Convergence test for (1.3a), $p = 2$, $\lambda = 0$, over the time interval $[0, 1]$.

J	h_{Γ^0}	(5.1) $\|\Gamma - \Gamma^h\|_{L^\infty}$	EOC	(5.2) $\|\Gamma - \Gamma^h\|_{L^\infty}$	EOC
32	2.1544e-01	2.1279e-03	—	2.2720e-03	—
64	1.0792e-01	5.3401e-04	2.00	5.6804e-04	2.01
128	5.3988e-02	1.3363e-04	2.00	1.4201e-04	2.00
256	2.6997e-02	3.3416e-05	2.00	3.5503e-05	2.00
512	1.3499e-02	8.3546e-06	2.00	8.8759e-06	2.00

TABLE 2
Convergence test for (1.3a), $p = 5$, $\lambda = 0$, over the time interval $[0, 1]$.

J	h_{Γ^0}	(5.1) $\|\Gamma - \Gamma^h\|_{L^\infty}$	EOC	(5.2) $\|\Gamma - \Gamma^h\|_{L^\infty}$	EOC
32	2.1544e-01	3.2297e-03	—	4.2993e-03	—
64	1.0792e-01	8.0173e-04	2.02	1.0631e-03	2.02
128	5.3988e-02	2.0008e-04	2.00	2.6507e-04	2.01
256	2.6997e-02	5.0001e-05	2.00	6.6227e-05	2.00
512	1.3499e-02	1.2499e-05	2.00	1.6554e-05	2.00

TABLE 3
Convergence test for (1.3a), $p = 1.1$, $\lambda = 0$, *over the time interval* $[0, 1]$.

		(5.1)		(5.2)	
J	h_{Γ^0}	$\|\Gamma - \Gamma^h\|_{L^\infty}$	EOC	$\|\Gamma - \Gamma^h\|_{L^\infty}$	EOC
32	2.1544e-01	8.9127e-04	—	1.4774e-04	—
64	1.0792e-01	2.2636e-04	1.98	3.7037e-05	2.00
128	5.3988e-02	5.6815e-05	2.00	9.2660e-06	2.00
256	2.6997e-02	1.4218e-05	2.00	2.3169e-06	2.00
512	1.3499e-02	3.5554e-06	2.00	5.7926e-07	2.00

For the choice (1.3b), we use a numerical solution of the differential equation (A.3) with (A.6), from the appendix, for (2.12) with $\lambda = 0$. For the presented convergence tests, we start with the initial data (6.1) with $r(0) = 0.5$. We compute the error (6.2) over the time interval $[0, 1]$. Here we use the time step size $\Delta t = 0.1 \, h_{\Gamma^0}^2$. For the choice $\alpha = 4$ the computed errors are reported in Table 4.

TABLE 4
Convergence test for (1.3b), $\alpha = 4$, $\lambda = 0$, *over the time interval* $[0, 1]$.

		(5.1)		(5.2)	
J	h_{Γ^0}	$\|\Gamma - \Gamma^h\|_{L^\infty}$	EOC	$\|\Gamma - \Gamma^h\|_{L^\infty}$	EOC
32	2.1544e-01	4.5099e-04	—	2.1356e-04	—
64	1.0792e-01	1.1368e-04	1.99	5.3519e-05	2.00
128	5.3988e-02	2.8479e-05	2.00	1.3156e-05	2.03
256	2.6997e-02	7.1234e-06	2.00	2.2891e-06	2.52
512	1.3499e-02	1.7811e-06	2.00	5.7227e-07	2.00

For (1.3c), we now investigate the behavior of circles close to stationary radial solutions with radius r such that $r^{-\frac{1}{2}} e^{-\alpha r} \left(\frac{1}{2} - \alpha r\right) + \lambda = 0$; recall (A.8) in the appendix. To this end, we numerically compute the stationary radius $r \approx 0.55617$ for $\alpha = 4$ and $\lambda = 0.25$; see Figure 11 (right). On noting (A.8) we observe that this stationary solution is stable. Indeed, starting with the initial data (6.1) with $r(0) = 0.4$ and $J = 128$, we use the scheme (5.2) to compute the evolution shown in Figure 1. Here we use the very small time step size $\Delta t = 10^{-7}$, since for larger values the Newton iteration to solve the nonlinear equations arising at each time step does not converge. With the chosen Δt, the maximum number of Newton iterations per time step was 2. We note that at the final time the discrete curve has a diameter of 1.112, which is approximately twice the expected radius of the stationary solution.
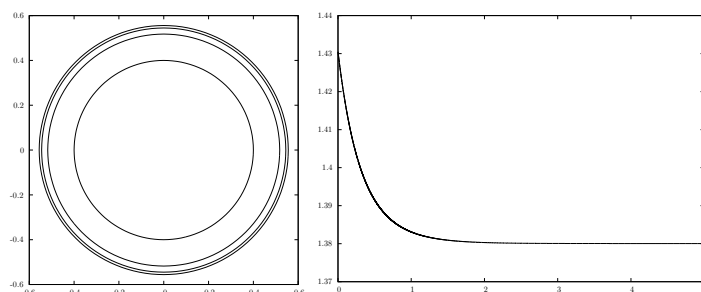

FIG. 1. (1.3c) *with* $\alpha = 4$, $\lambda = 0.25$. *Left: Plots of the curve at times* $t = 0, 1, 2, 5$. *Right:* t *versus discrete energy on* $[0, 5]$.

6.1.2. Clamped boundary conditions. In order to test the convergence of the schemes in the presence of clamped boundary conditions, we consider the stable stationary solution for (1.3a) with $r = 1$ and $\lambda = \frac{p-1}{p}$; recall (A.8) in the appendix. Similarly to (6.1), we choose the initial data

$$\vec{X}^0(q_j) = \begin{pmatrix} \sin[(q_j - \frac{1}{2})\,\pi + 0.1\,\cos((q_j - \frac{1}{2})\,\pi)] \\ \cos[(q_j - \frac{1}{2})\,\pi + 0.1\,\cos((q_j - \frac{1}{2})\,\pi)] \end{pmatrix}, \quad j = 0, \ldots, J,$$

and provide the boundary conditions defined by X^0 and $\vec{\zeta}_0 = \vec{\zeta}_1 = -\vec{e}_2$. On computing the solution until time $t = 1$, with $\Delta t = 0.1\,h_{\Gamma^0}^2$, we compute the maximal distance between $\vec{X}^M(q_j)$ and the unit semicircle. For the choice $p = 4$, the results are presented in Table 5. As we start the simulations with an interpolation of the true steady state solution, we observe some superconvergence for large h_{Γ^0}. But eventually the convergence rates seem to settle on second order.

TABLE 5
Convergence test for clamped boundary conditions for (1.3a), $p=4$, *with* $\lambda = \frac{3}{4}$ *and* $\vec{\zeta}_0 = \vec{\zeta}_1 = -\vec{e}_2$.

		(5.1)		(5.2)	
J	h_{Γ^0}	$\|\Gamma(1) - \Gamma^M\|$	EOC	$\|\Gamma(1) - \Gamma^M\|$	EOC
32	1.0792e-01	3.0545e-05	—	2.7926e-05	—
64	5.3988e-02	4.1892e-06	2.87	3.6824e-06	2.93
128	2.6997e-02	6.1270e-07	2.77	5.0761e-07	2.86
256	1.3499e-02	9.9239e-08	2.63	7.5317e-08	2.75
512	6.7495e-03	1.8154e-08	2.45	1.2393e-08	2.60

For the same setup as for Table 5, we now present a simulation each with $\lambda < \frac{3}{4}$ and $\lambda > \frac{3}{4}$, so that the unit semicircle is no longer a stationary solution. The plots of the obtained numerical steady state solutions, for the scheme (5.2) with $J = 128$ and $\Delta t = 10^{-3}$, are shown in Figure 2.
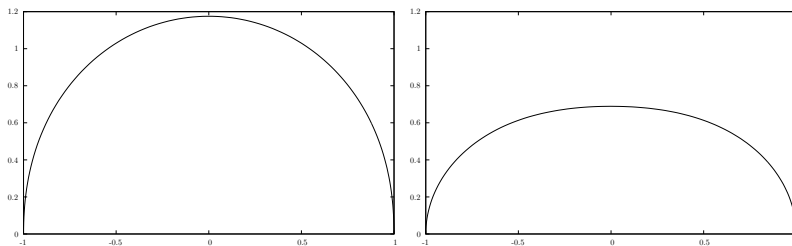

FIG. 2.   *Steady state solutions for* (1.3a) *with* $p = 4$ *and clamped boundary conditions* $\vec{\zeta}_0 = \vec{\zeta}_1 = -\vec{e}_2$. *Left:* $\lambda = 0.01$. *Right:* $\lambda = 10$.

In the next experiment, we connect two horizontal lines by a minimizing curve. In Figure 3, we show the comparison of the obtained discrete approximations to the minimizers for the energy (2.5), with $\lambda = 0.1$, for (1.3a) with $p \in \{1.6, 2, 4, 15\}$. Here we use the scheme (5.2) with $J = 128$ and $\Delta t = 10^{-5}$. We note that for $p < 2$ the steady state solution becomes more straight, while for $p > 2$ the shape is more curved. In other words, for $p < 2$ the maximal curvature and the length of the curve become smaller, while for $p > 2$ both become larger. The discrete energies for the displayed solutions are 0.963, 0.791, 0.421, and 0.236, respectively.

In order to allow simulations of the situation in Figure 3 for the choice (1.3b), we apply a regularization term and consider
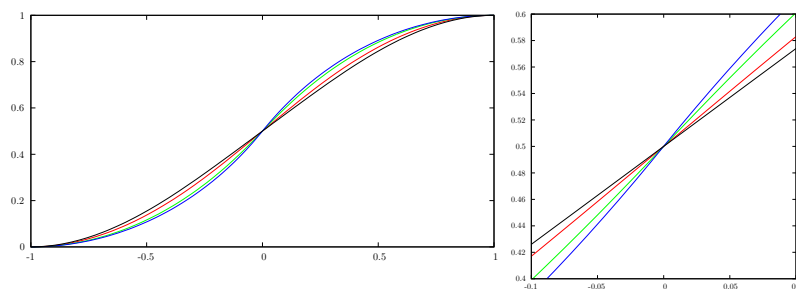
FIG. 3. *Steady state solutions for* (1.3a) *with* $p = 1.6$ *(black),* $p = 2$ *(red),* $p = 4$ *(green) and* $p = 15$ *(blue),* $\lambda = 0.1$ *and clamped boundary conditions* $\vec{\zeta}_1 = -\vec{\zeta}_0 = \vec{e}_1$. *A closeup around the point* $(0, 0.5)^T$ *on the right. Color refers to online figures.*

$$(6.3) \qquad G(z) = e^{-\alpha/z} + \tfrac{1}{2}\,\varepsilon\,z^2 \quad \text{with } \varepsilon = 10^{-12}\,.$$

This is purely to help overcome numerical difficulties when $|z|$ is small, and, as far as we can establish, this has no major influence on the computed evolution. For example, the errors in Table 4 for the scheme (5.2), but with (1.3b) replaced by (6.3), are given by 2.1361e-04, 5.3522e-05, 1.3388e-05, 3.3475e-06, 8.3687e-07. In Figure 4, we show the comparison of the obtained discrete approximations to the minimizers for the energy (2.5), with $\lambda = 0.1$, for (6.3) with $\alpha \in \{3, 4, 9, 15\}$. Here we use the scheme (5.2) with $J = 128$ and $\Delta t = 10^{-5}$. We observe that, in contrast to Figure 3, the arrangements of the stationary curves is not monotone in the parameter α. In particular, the curve for $\alpha = 3$ lies between the curves for $\alpha = 4$ and $\alpha = 9$. In fact, further numerical investigations suggest that $\alpha = 4$ is approximately the value that leads to the largest deformation of the stationary curve. The discrete energies for the solutions displayed in Figure 4 are 0.271, 0.243, 0.228, and 0.226, respectively.
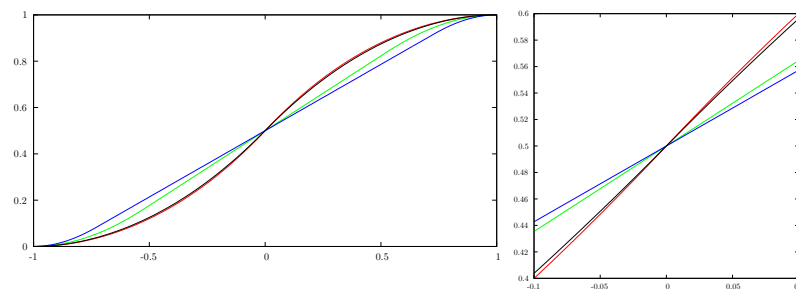

FIG. 4. *Left: Steady state solutions for* (6.3) *with* $\alpha = 3$ *(black),* $\alpha = 4$ *(red),* $\alpha = 9$ *(green) and* $\alpha = 15$ *(blue),* $\lambda = 0.1$ *and clamped boundary conditions* $\vec{\zeta}_1 = -\vec{\zeta}_0 = \vec{e}_1$. *Right: A closeup around the point* $(0, 0.5)^T$. *Color refers to online figures.*

6.2. Numerical results for $d = 3$. Here we only consider clamped boundary conditions, since we expect stationary closed curves to lie within two-dimensional hyperplanes. Throughout this subsection, we let $\lambda = 1$ and choose the discretization parameters $J = 512$ and $\Delta t = 10^{-4}$. Unless otherwise stated, we employ the scheme (5.2).

We begin with an evolution for a segment of a helix, parameterized by $\vec{x}_0(\rho) = \left[\rho, \sin(2\,\pi\rho), \cos(2\,\pi\,\rho)\right]^T$ for $\rho \in [0, 1]$, for the clamped boundary conditions (2.3) given by $\vec{x}_0$ and $\vec{\zeta}_1 = -\vec{\zeta}_0 = \vec{e}_2$. For the energy induced by (1.3a) with $p = 1.5$,
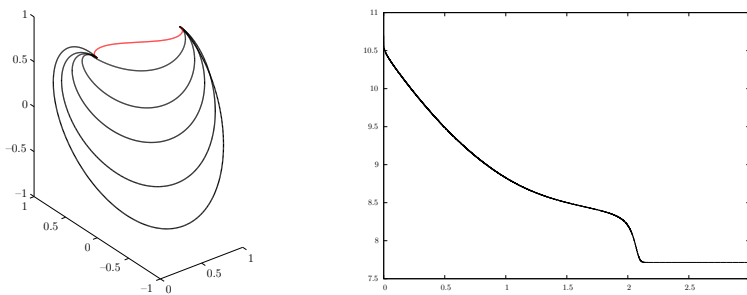
FIG. 5. *Evolution of a helical curve.* (1.3a) *with* $p = 1.5$, $\lambda = 1$, $\vec{\zeta}_1 = -\vec{\zeta}_0 = \vec{e}_2$. *Left: Plots of the curve at times* $t = 0, 0.5, \ldots, 2.5$, *with the almost stationary (planar) curve at time* $t = 2.5$ *in red. Right: t versus discrete energy on* $[0, 3]$. *Color refers to online figures.*

the initially three-dimensional curve collapses to a curve that lies in a hyperplane parallel to the $x - y$–plane. See Figure 5 for the evolution. The energy plot nicely illustrates the rapid decay of the energy as the curve settles into the two-dimensional hyperplane, where it appears to have reached a steady state. The discrete energy for the final solution in Figure 5 is 7.71.

For (1.3a) with $p \in \{2, 4, 15\}$, however, the curve remains three-dimensional throughout, until it settles on a stationary shape; see Figure 6. Similarly to Figure 3, we observe that larger values of p lead to curves with higher maximal curvature and greater overall length. The discrete energies for the solutions displayed in Figure 6 are 8.67, 7.70, and 6.65, respectively. We remark that starting the evolution from the final shape in Figure 5, for $p = \{2, 4, 15\}$, still leads to the stationary solutions displayed in Figure 6. Hence we conjecture that these solutions are indeed discrete approximations to the global minimizer for the considered curvature energy and the prescribed clamped boundary conditions.
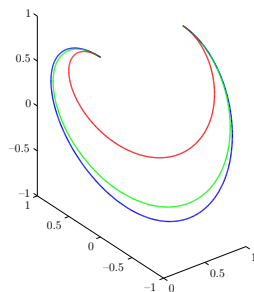

FIG. 6. *Nonplanar steady state solutions for* (1.3a) *with* $\lambda = 1$, $\vec{\zeta}_1 = -\vec{\zeta}_0 = \vec{e}_2$ *and* $p = 2$ *(red)*, $p = 4$ *(green) and* $p = 15$ *(blue). Color refers to online figures.*

Moreover, we conjecture that the global minimizer changes from a planar to a nonplanar shape for a critical value of p. As an explanation we can state that for the given setup the curvature's contribution to the energy, $\frac{1}{p} \int |\vec{\varkappa}|^p$, for any planar connection between the two clamped endpoints increases strongly with p, and it will start to dominate the term that penalizes the length of the curve. Eventually, for p sufficiently large, a longer, nonplanar, circle-like connection will have a smaller overall energy $\int [\frac{1}{p} |\vec{\varkappa}|^p + 1]$. To study this further, we computed for a set of p values in $[1.5, 2]$, and for two possible initial curves (either planar (two-dimensional), or
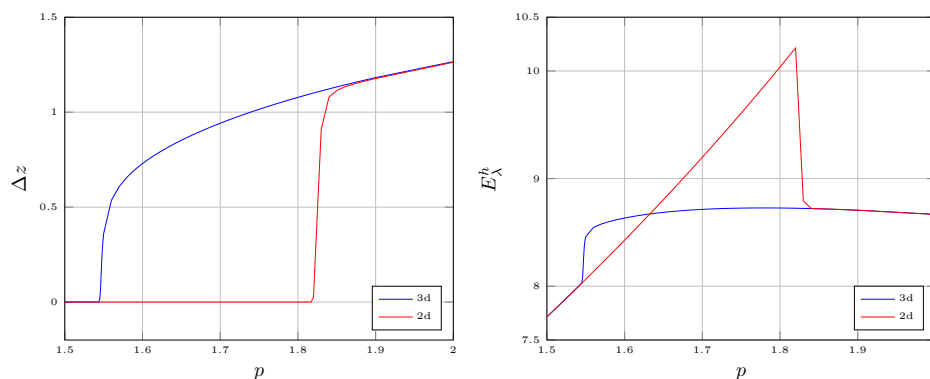
FIG. 7. *A plot of* $\Delta z = \max_{j,\ell=0,\ldots,J} |(\vec{X}^M(q_j) - \vec{X}^M(q_\ell)) \cdot \vec{e}_3|$ *(left) and the discrete energy* E_λ^h *(right) against* p *in* (1.3a). *Here we show a curve each for two-dimensional (red) and three-dimensional (blue) initial data, respectively. Color refers to online figures.*

nonplanar (three-dimensional)), the diameter in z-direction of the stationary solution; see Figure 7. It can be seen that for values $p \in [1.55, 1.81]$, two different stationary states appear to exist (planar and nonplanar), and the initial data critically determines which state is reached. Moreover, by comparing the energy of the final states, we conjecture that the planar stationary state is the minimizer for $p < 1.63$, while the nonplanar curve is the minimizer for $p > 1.64$.

We remark that the scheme (5.1) is not able to integrate the evolution in Figure 5 with the same discretization parameters. Even if we choose the much smaller time step size $\Delta t = 10^{-6}$, the scheme (5.1) can only compute the evolution until about $t = 1.4$, at which point the scheme breaks down due to coalescence of mesh points. In Figure 8 we compare the element ratio

$$(6.4) \qquad \mathfrak{r}^m = \frac{\max_{j=1 \to J} |\vec{X}^m(q_j) - \vec{X}^m(q_{j-1})|}{\min_{j=1 \to J} |\vec{X}^m(q_j) - \vec{X}^m(q_{j-1})|}$$

for the schemes (5.1) and (5.2) for this simulation with $\Delta t = 10^{-6}$ until time $t = 1$. It can be clearly seen that for the scheme (5.1) the ratio increases dramatically, while for the scheme (5.2) the ratio converges to 1, meaning an equidistribution of the vertices.

Finally, for (1.3a) with $p \in \{1.5, 4\}$, we show some more involved evolutions towards the steady states shown in Figures 5 and 6. To this end, we choose as initial data a discretisation of

$$\vec{x}_0(\rho) = \left[\rho, \sin(4\,\pi\rho), \cos(4\,\pi\,\rho)\right]^T \qquad \forall\, \rho \in [0, 1],$$

i.e., a helix with two turns. The computed evolutions are shown in Figures 9 and 10.
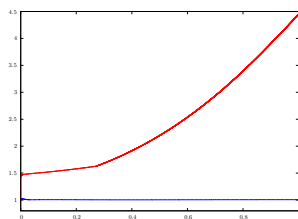

FIG. 8. *The time evolution of the ratio* (6.4) *for the schemes* (5.1) *(red) and* (5.2) *(blue) for the experiment as in* FIG. 5 *with* $\Delta t = 10^{-6}$. *Color refers to online figures.*
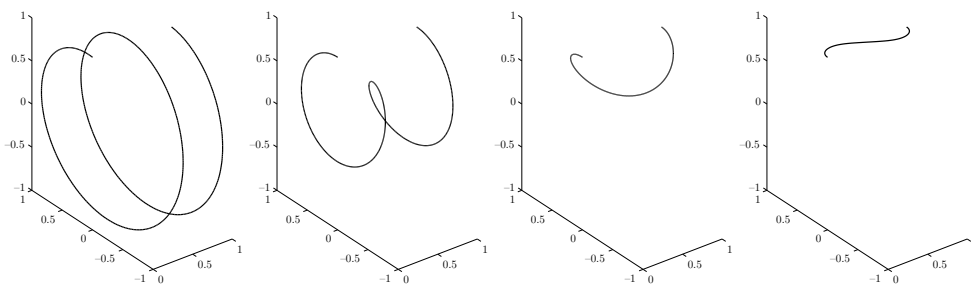
FIG. 9. *Evolution of a double-winded helical curve.* (1.3a) *with* $p = 1.5$, $\lambda = 1$, $\vec{\zeta}_1 = -\vec{\zeta}_0 = \vec{e}_2$. *The convergence is towards the steady state solution shown in* FIG. 5. *The curve is shown at times* $t = 0, 1, 2, 5$ *(from left to right).*
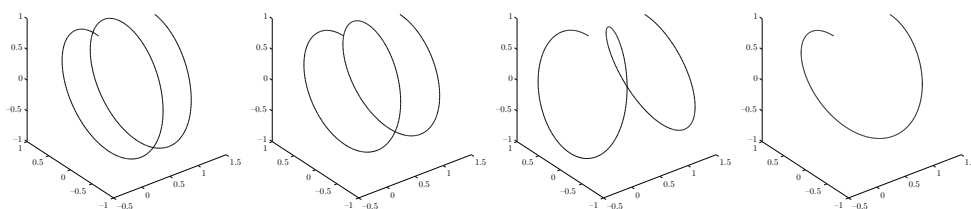

FIG. 10. (1.3a) *with* $p = 4$, $\lambda = 1$, $\vec{\zeta}_1 = -\vec{\zeta}_0 = \vec{e}_2$. *Evolution of a clamped helix towards the steady state solution shown in* FIG. 6. *The curve is shown at times* $t = 0, 5, 10, 20$.

Conclusion. We have presented two continuous-in-time semidiscrete finite element discretizations for the approximation of the L^2-gradient flow of general curvature energies of the form (2.5), featuring a general energy density G. Here we have considered closed and open curves, taking into account clamped boundary conditions in the case of open curves. Both schemes can be shown to be stable, and the second variant satisfies, in addition, an equidistribution property. The introduced corresponding fully discrete approximations, (5.1) and (5.2), are in general mildly nonlinear, due to the possible nonlinearities present in G'. In practice both schemes perform well in convergence tests, using exact radial solutions developed in the appendix and exhibit good stability properties. The scheme (5.2) proved to be more robust in practice, as (5.1) could at times not compute evolutions unless the time discretization parameter was chosen sufficiently small. Moreover, the scheme (5.1) can suffer from coalescence in practice, while the vertices for scheme (5.2) are always well distributed.

Appendix A. Exact radial solutions for $d = 2$.

General planar curves. For a closed curve in the case $d = 2$ we can define the normal to the curve via $\vec{\nu} = -\vec{\tau}^{\perp}$, where $(\cdot)^{\perp}$ denotes a clockwise rotation by $\frac{\pi}{2}$. Then we can introduce the curve's scalar curvature via

$$(A.1) \qquad \varkappa \vec{\nu} = \vec{\varkappa} = \vec{\tau}_s = \vec{x}_{ss};$$

see, e.g., [10]. On noting that

$$\vec{\nabla}_s^2 \left(G'(|\vec{\varkappa}|) \, |\vec{\varkappa}|^{-1} \, \vec{\varkappa} \right) = \vec{\nabla}_s^2 \left(G'(|\varkappa|) \, |\varkappa|^{-1} \, \varkappa \vec{\nu} \right) = \left[\left(G'(|\varkappa|) \, |\varkappa|^{-1} \, \varkappa \vec{\nu} \right)_s \cdot \vec{\nu} \, \vec{\nu} \right]_s \cdot \vec{\nu} \, \vec{\nu}$$
$$= \left[\left(G'(|\varkappa|) \, |\varkappa|^{-1} \, \varkappa \right)_s \vec{\nu} \right]_s \cdot \vec{\nu} \, \vec{\nu} = \left(G'(|\varkappa|) \, |\varkappa|^{-1} \, \varkappa \right)_{ss} \vec{\nu},$$

it is straightforward to establish that (2.13), for $d = 2$, can be formulated as

$$(A.2) \qquad \vec{x}_t \cdot \vec{\nu} = -(G'(|\varkappa|)\,|\varkappa|^{-1}\,\varkappa)_{ss} + \left[G(|\vec{\varkappa}|) - G'(|\varkappa|)\,|\varkappa|\right]\varkappa + \lambda\,\varkappa.$$

For the special case (1.3a) with $p = 2$, (A.2) reduces to $\vec{x}_t \cdot \vec{\nu} = -\varkappa_{ss} - \frac{1}{2}\,\varkappa^3 + \lambda\,\varkappa$, the standard elastic flow in the plane.

We now make the ansatz

$$(A.3) \qquad \vec{x}(\rho, t) = r(t)\left[\cos(2\pi\rho)\,\vec{e}_1 + \sin(2\pi\rho)\,\vec{e}_2\right] \qquad \forall\,\rho \in I\,,$$

with $r(t) > 0$ for all $t \in [0, T]$. It follows from (A.1) that $\varkappa(\rho, t) = [r(t)]^{-1}$ and $\vec{x}_t(\rho, t) \cdot \vec{\nu}(\rho, t) = -r'(t)$, for all $\rho \in I$ and $t \in [0, T]$. Hence a solution of the form (A.3) for the flow (A.2) needs to satisfy

$$(A.4) \qquad \frac{1}{2}\frac{\mathrm{d}}{\mathrm{d}t}\,r^2(t) = G'\!\left(\tfrac{1}{r(t)}\right)\frac{1}{r(t)} - G\!\left(\tfrac{1}{r(t)}\right) - \lambda\,.$$

The case (1.3a). Here we obtain the ordinary differential equation

$$\frac{1}{2}\frac{\mathrm{d}}{\mathrm{d}t}\,r^2(t) = \left[\tfrac{1}{r(t)}\right]^{p-1}\frac{1}{r(t)} - \frac{1}{p}\left[\tfrac{1}{r(t)}\right]^p - \lambda = \left(1 - \tfrac{1}{p}\right)\left[\tfrac{1}{r(t)}\right]^p - \lambda\,.$$

It is easy to verify that the solution in the case of $\lambda = 0$ is

$$(A.5) \qquad r(t) = \left[\tfrac{(p-1)\,(p+2)}{p}\,t + r(0)^{p+2}\right]^{\frac{1}{p+2}}\,.$$

In particular, for $p \in (1, \infty)$, the solution (A.5) represents expanding circles. For $p = 2$, we obtain the well-known expanding circle solution with radius $r(t) = (2\,t + r(0)^4)^{\frac{1}{4}}$ for the elastic flow in the plane.

The case (1.3b). The differential equation (A.4) implies

$$\frac{1}{2}\frac{\mathrm{d}}{\mathrm{d}t}\,r^2(t) = (\alpha\,r(t) - 1)\,e^{-\alpha\,r(t)} - \lambda\,,$$

which for $\lambda = 0$ yields

$$(A.6) \qquad r'(t) = \left(\alpha - \tfrac{1}{r(t)}\right)e^{-\alpha\,r(t)}\,.$$

We note that a circle with radius $r = \frac{1}{\alpha}$ is an unstable steady state solution to (A.6); see also the final paragraph below. Circles with a larger radius will (unboundedly) expand, while circles with a smaller radius will shrink (to 0).

If we let $A'(y) = y\,[\alpha\,y - 1]^{-1}\,e^{\alpha\,y}$, we find its antiderivative to be $A(y) = \alpha^{-2}\left(e\,\mathrm{Ei}(\alpha\,y - 1) + e^{\alpha\,y}\right)$, where $\mathrm{Ei}(z) = -\int_{-z}^{\infty} u^{-1}\,e^{-u}\,\mathrm{d}u$ denotes the well-known exponential integral. Then a solution to (A.6), with $r(t) > \frac{1}{\alpha}$, satisfies $\frac{\mathrm{d}}{\mathrm{d}t}\,A(r(t)) = r'(t)\,A'(r(t)) = 1$, which means that a solution to (A.6) satisfies the nonlinear equation

$$A(r(t)) = t + A(r(0))\,,$$

which can be solved numerically to find $r(t)$.

The case (1.3c). The differential equation (A.4) implies

$$\frac{1}{2}\frac{\mathrm{d}}{\mathrm{d}t}\,r^2(t) = \left(\alpha\,r(t) - \tfrac{1}{2}\right)\left[\tfrac{1}{r(t)}\right]^{\frac{1}{2}}e^{-\alpha\,r(t)} - \lambda\,,$$

which for $\lambda = 0$ yields

$$(A.7) \qquad r'(t) = \left(\alpha - \tfrac{1}{2}\tfrac{1}{r(t)}\right)\left[\tfrac{1}{r(t)}\right]^{\frac{1}{2}}e^{-\alpha\,r(t)}\,.$$

We note that a circle with radius $r = \frac{1}{2\,\alpha}$ is an unstable steady state solution to (A.7); see also the final paragraph below. Circles with a larger radius will expand, while circles with a smaller radius will shrink.

Stability of stationary solutions. We observe that for our examples in (1.3) circles of radius $r = |\vec{x}|$ have energy

$$E_\lambda(\vec{x}) = 2\,\pi\left(G\big(\tfrac{1}{r}\big) + \lambda\right) r = 2\,\pi\,g_\lambda(r), \quad g_\lambda(r) = \begin{cases} \frac{1}{p}\,r^{1-p} + \lambda\,r & \text{(1.3a)}, \\ r\,e^{-\alpha\,r} + \lambda\,r & \text{(1.3b)}, \\ \sqrt{r}\,e^{-\alpha\,r} + \lambda\,r & \text{(1.3c)}. \end{cases}$$

In particular, if $r \to 0$, then only in the case (1.3a) the energy grows unbounded. For the other two cases, circles with radius $r \to 0$ are a minimizing sequence for (2.5) if $\lambda \geq 0$.

The radii of stationary radial solutions are now simply the stationary points of g_λ. Their stability can be inferred from the sign change of g_λ', or from the sign of g_λ'', where

(A.8)

$$g_\lambda'(r) = \begin{cases} \frac{1-p}{p}\,r^{-p} + \lambda, \\ e^{-\alpha\,r}\,(1 - \alpha\,r) + \lambda, \\ r^{-\frac{1}{2}}\,e^{-\alpha\,r}\,(\frac{1}{2} - \alpha\,r) + \lambda, \end{cases} \quad \text{and} \quad g_\lambda''(r) = \begin{cases} (p-1)\,r^{-(p+1)} & \text{(1.3a)}, \\ \alpha\,e^{-\alpha\,r}\,(\alpha\,r - 2) & \text{(1.3b)}, \\ r^{-\frac{3}{2}}\,e^{-\alpha\,r}\,(\alpha\,r^2 - \alpha\,r - \frac{1}{4}) & \text{(1.3c)}. \end{cases}$$

In particular, if r is the radius of a stationary radial solution, i.e., $g_\lambda'(r) = 0$, then for (1.3a) this stationary solution is always stable. For the choice (1.3b) it is stable if $r > \frac{2}{\alpha}$, while for (1.3c) it is stable if $r > \frac{1}{2}\,([1 + \frac{1}{\alpha}]^{\frac{1}{2}} - 1)$. We reformulate the equation $g_\lambda'(r) = 0$ for the stationary radii in the form $f(r, \alpha) = \lambda$ (for examples (1.3b) and (1.3c)) and provide the graph of $f(\cdot, \alpha)$ in Figure 11 for some values of α. It can be seen that there exist no stationary solutions for the cases (1.3b) and (1.3c) and the chosen values of α if $\lambda > 0$ is too large.

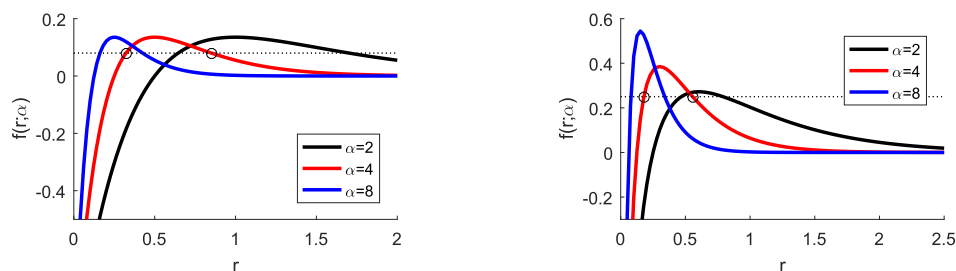

FIG. 11. *Stationary radial solutions as the intersection of $f(\cdot, \alpha)$, for $\alpha \in \{2, 4, 8\}$, with the line $\lambda = const$ (dotted line). The two solutions for $\alpha = 4$ are marked with a circle. The left solution is unstable while the right one is stable. Note that there are no stationary solutions for even moderate $\lambda > 0$. Left: Example (1.3b) with $\lambda = 0.08$. Right: Example (1.3c) with $\lambda = 0.25$. Color refers to online figures.*

REFERENCES

[1] R. BAETS AND P. E. LAGASSE, *Loss calculation and design of arbitrarily curved integrated-optic waveguides*, J. Opt. Soc. Amer., 73 (1983), pp. 177–182.

[2] J. W. BARRETT, H. GARCKE, AND R. NÜRNBERG, *Numerical approximation of gradient flows for closed curves in $\mathbb{R}^d$*, IMA J. Numer. Anal., 30 (2010), pp. 4–60.

[3] J. W. BARRETT, H. GARCKE, AND R. NÜRNBERG, *The approximation of planar curve evolutions by stable fully implicit finite element schemes that equidistribute*, Numer. Methods Partial Differential Equations, 27 (2011), pp. 1–30.

[4] J. W. BARRETT, H. GARCKE, AND R. NÜRNBERG, *Parametric approximation of isotropic and anisotropic elastic flow for closed and open curves*, Numer. Math., 120 (2012), pp. 489–542.

[5] S. BARTELS, *A simple scheme for the approximation of the elastic flow of inextensible curves*, IMA J. Numer. Anal., 33 (2013), pp. 1115–1125.

[6] S. BARTELS, P. REITER, AND J. RIEGE, *A simple scheme for the approximation of self-avoiding inextensible curves*, IMA J. Numer. Anal., 38 (2018), pp. 543–565.

[7] A. DALL'ACQUA, C.-C. LIN, AND P. POZZI, *A gradient flow for open elastic curves with fixed length and clamped ends*, Ann. Sc. Norm. Super. Pisa Cl. Sci. 17 (2017), pp. 1031–1066.

[8] T. A. DAVIS, *Algorithm 832: UMFPACK V4.3—an unsymmetric-pattern multifrontal method*, ACM Trans. Math. Softw., 30 (2004), pp. 196–199.

[9] K. DECKELNICK AND G. DZIUK, *Error analysis for the elastic flow of parametrized curves*, Math. Comp., 78 (2009), pp. 645–671.

[10] K. DECKELNICK, G. DZIUK, AND C. M. ELLIOTT, *Computation of geometric partial differential equations and mean curvature flow*, Acta Numer., 14 (2005), pp. 139–232.

[11] K. DECKELNICK AND H.-C. GRUNAU, *Boundary value problems for the one-dimensional Willmore equation*, Calc. Var. Partial Differential Equations, 30 (2007), pp. 293–314.

[12] K. DECKELNICK AND H.-C. GRUNAU, *Stability and symmetry in the Navier problem for the one-dimensional Willmore equation*, SIAM J. Math. Anal., 40 (2009), pp. 2055–2076.

[13] G. DZIUK, *An algorithm for evolutionary surfaces*, Numer. Math., 58 (1991), pp. 603–611.

[14] G. DZIUK, *Convergence of a semi-discrete scheme for the curve shortening flow*, Math. Models Methods Appl. Sci., 4 (1994), pp. 589–606.

[15] G. DZIUK, *Computational parametric Willmore flow*, Numer. Math., 111 (2008), pp. 55–80.

[16] G. DZIUK, E. KUWERT, AND R. SCHÄTZLE, *Evolution of elastic curves in $\mathbb{R}^n$: Existence and computation*, SIAM J. Math. Anal., 33 (2002), pp. 1228–1245.

[17] L. EULER, *Opera Omnia, Ser.* 1, Orell Füssli, Zurich, 1952.

[18] S. GOYAL, N. C. PERKINS, AND C. L. LEE, *Nonlinear dynamics and loop formation in Kirchhoff rods with implications to the mechanics of DNA and cables*, J. Comput. Phys., 209 (2005), pp. 371–389.

[19] C. KOOS, C. G. POULTON, L. ZIMMERMANN, L. JACOME, J. LEUTHOLD, AND W. FREUDE, *Ideal bend contour trajectories for single-mode operation of low-loss overmoded waveguides*, IEEE Photon. Technol. Lett., 19 (2007), pp. 819–821.

[20] N. LINDENMANN, G. BALTHASAR, D. HILLERKUSS, R. SCHMOGROW, M. JORDAN, J. LEUTHOLD, W. FREUDE, AND C. KOOS, *Photonic wire bonding: A novel concept for chip-scale interconnects*, Opt. Express, 20 (2012), pp. 17667–17677.

[21] D. MARCUSE, *Bend loss of slab and fiber modes computed with diffraction theory*, IEEE J. Quantum Electron., 29 (1993), pp. 2957–2961.

[22] W. MIO, A. SRIVASTAVA, AND E. KLASSEN, *Interpolations with elasticae in Euclidean spaces*, Quart. Appl. Math., 62 (2004), pp. 359–378.

[23] F. NEGREDO, M. BLAICHER, A. NESIC, P. KRAFT, J. OTT, W. DÖRFLER, C. KOOS, AND C. ROCKSTUHL, *Fast and reliable method to estimate losses of single-mode waveguides with an arbitrary 2D trajectory*, J. Opt. Soc. Am. A, 35 (2018), pp. 1063–1073.

[24] A. POLDEN, *Curves and surfaces of least total curvature and fourth-order flows*, PhD thesis, University Tübingen, Tübingen, 1996.

[25] R. SCHÄTZLE, *The Willmore boundary problem*, Calc. Var. Partial Differential Equations, 37 (2010), pp. 275–302.

[26] A. SCHMIDT AND K. G. SIEBERT, *Design of Adaptive Finite Element Software: The Finite Element Toolbox ALBERTA*, Lecture Notes in Computational Science and Engineering 42, Springer-Verlag, Berlin, 2005.

[27] F. TRÖLTZSCH, *Optimal Control of Partial Differential Equations: Theory, Methods and Applications*, Graduate Studies in Mathematics 112, AMS, Providence, RI, 2010.

[28] Z. C. TU AND Z. C. OU-YANG, *Elastic theory of low-dimensional continua and its applications in bio- and nano-structures*, J. Comput. Theor. Nanosci., 5 (2008), pp. 422–448.